Scientific Research Publishing

Journal of Modern Physics, 2021, 12, 1483-1517
https://www.scirp.org/journal/jmp
ISSN Online: 2153-120X
ISSN Print: 2153-1196

Cosmological Tests of the Hypothesis of Dark Matter as Bound Neutrinos

Richard B. Holmes

nLIGHT|Nutronics, Vancouver, USA
Email: rholmes001@aol.com

How to cite this paper: Holmes, R.B. (2021) Cosmological Tests of the Hypothesis of Dark Matter as Bound Neutrinos. *Journal of Modern Physics*, **12**, 1483-1517.
https://doi.org/10.4236/jmp.2021.1211090

Received: July 15, 2021
Accepted: September 6, 2021
Published: September 9, 2021

Abstract

A modest extension of the Standard Model allows a family-specific, feeble form of SU(3) that causes rapid binding of neutrinos at neutrino decoupling. These bound neutrinos become nonrelativistic well before recombination. Neutrinos are bound when all three neutrino flavors are present at densities expected in the early universe. Consistency is examined against observationally-inferred data, including free-streaming lengths, dark matter interaction rates, neutrinos from SN1987A, big-bang nucleosynthesis, and the cosmic microwave background. Consistency with galactic haloes and halo interactions was studied in a companion paper. The theory yields a ratio of dark matter density to neutrino density of 147, calculated in two different ways, agreeing with the current value of 158 assuming the sum of the masses of neutrino mass eigenstates is 0.07 eV/c^2. This yields a ratio of dark matter to total matter of 83.2% with a relative uncertainty of at least ±8%. A free-streaming length of about 1 kpc is obtained for hard-sphere self-scattering, and about 115 kpc for $1/r$-potential self-scattering, where r is the particle separation. A BBN analysis agrees with observationally-inferred abundances of He and Li, but not the latest deuterium measurements. The latter disagreement is the only identified potential inconsistency with current cosmological measurements. Both the standard SU(3) adapted to the neutrino family and a modest extension of SU(3) give good agreement with most observations. The extension provides a means to estimate dark matter parameters whereas the standard SU(3) does not. This explanation for dark matter does not require any new fundamental particles or forces.

Keywords

Dark Matter, Neutrinos, Cosmology

1. Introduction

The conventional picture of neutrinos as dark matter (DM) was ruled out early

[1] because the corresponding large free-streaming scale length of such particles is not consistent with the observed structure of the modern universe. The best current model for DM is the Λ-CDM model [2] [3] which assumes a certain fraction of the matter in the universe is cold (nonrelativistic), non-interacting, and stable [4]. However, this model provides no explanation for the nature of dark matter, and consistency with galactic-scale haloes is not evident. There have been many hypothetical explanations for dark matter. Of most relevance are those involving some form of warm dark matter (WDM) [5]. As early as 2000, it was written that "it is clear that there is an (over) abundance of mechanisms for producing warm dark matter, using modest extensions of physics beyond the Standard Model [6]". In this paper, yet another modest extension of the Standard Model is investigated as an explanation for DM as a form of WDM. This extension utilizes neutrinos, assuming the sum of the masses of neutrino mass eigenstates is 0.07 eV/c^2, and a feeble form of SU(3). This feeble form of SU(3) results in a neutrino equivalent of a phase transition from a quark-gluon plasma to a hot hadron gas in the early universe. This both cools the neutrino sector and creates larger-mass particles. It also results in diffusive transport of matter rather than ballistic transport after the phase transition. This phase transition combined with diffusive transport results in dramatically smaller scale lengths for neutrino streaming in the early universe, as will be seen below.

The standard view of dark matter posits that DM was in thermal contact with ordinary matter (OM) in the early universe when the temperature was much greater than the DM mass. In that era, the DM number density would be comparable to photon number density. If the DM number density were still comparable to the photon number density when it froze out, it would overproduce the observed amount of DM mass for particles with masses greater than about 1 eV/c^2. Hence there is a need to deplete such matter, presumably by annihilation. This is the path that leads to CDM particles that are largely annihilated in the early universe. With kT~100 GeV, where k is Boltzmann's constant and T is the temperature, one obtains a weak interaction cross-section that when multiplied by the density and velocity at that time results in a decay rate comparable to the expansion rate. This would result in freeze-out at that time in the early universe for the corresponding particle mass. Hence DM masses of order 100 GeV are candidates for DM under these standard assumptions. These would become cold (nonrelativistic) over the eons as the universe expanded.

With the absence of significant evidence of massive candidate particles for DM, the community is looking to lighter alternatives. Most recent papers consider particles with masses of the order of a few keV, as is consistent with observationally-inferred values from the latest Lyman-α forest absorption measurements [7] and gravitational lensing measurements [8], based on various assumptions. These assumptions are inconsistent with the form of dark matter considered here, in which light matter binds into a number of species of heavier particles shortly after neutrino decoupling, which then further binds into macros-

copic structures well before recombination. Such self-interacting DM (SIDM) avoids the free-streaming issue with lighter DM as shown below.

In the past 4 decades, computationally-intensive approaches have investigated the consistency of lighter DM with astronomical observations. Such investigations began with [1] regarding the possibility of neutrinos for dark matter. Hernquist *et al.* [9] investigated consistency of dark matter with Lyman-α lines. Early modeling of self-interacting DM includes papers on elastic collisions [10], on gravothermal collapse [11], and on subhaloes [12]. Shao *et al.* [13] addressed the impact of fermions. More recently, [14] [15] performed extensive modeling of galaxy formation within larger structures in the universe. Cyr-Racine *et al.* [16] investigated an effective theory for small scale structure. Robertson *et al.* [17] [18] considered SIDM and halo interactions, [19] considered the impact of SIDM on structure and self-assembly history, and [20] modeled SIDM that includes inelastic scattering. There has been a recent review of SIDM [21], and of the larger topic of dark matter haloes and subhaloes [22].

An earlier, companion paper [23] addressed the consistency of the proposed form of dark matter with galactic haloes. That paper found quantitative agreement with observationally-inferred sizes, shapes, and masses of DM haloes of the size of the Milky Way halo or smaller. It also found quantitative consistency of the proposed form of dark matter with the observed delay between ordinary matter and dark matter for the Bullet cluster interaction. It further provided semi-quantitative explanations for halo stability, halo cores and cusps, and for the observationally-inferred paucity of smaller haloes.

This paper presents the cosmological consequences of a neutrino self-interaction based on SU(3) adapted to the neutrino family, with estimates for interaction strengths and binding energies derived from an extended form of SU(3) given in [24]. This form of SU(3) will be denoted "$SU(3)_{ve}$." The standard SU(3) adapted to the neutrino family will be denoted "$SU(3)_{vs}$". It should be emphasized that a neutrino SU(3) should not occur in the Standard Model, because in an SU(3) × $[SU(2)_L \times U(1)]$ model, a neutrino SU(3) would imply an electron SU(3), which is contrary to evidence. However, in this theory, linear combinations of neutrinos form extended-color (EC) singlets which pair with corresponding electron-family EC singlets in the electroweak Lagrangian via a non-trivial Pontecorvo-Maki-Nakagawa-Sakata (PMNS) matrix. Further, the theory is anomaly-free and renormalizable [25]. Other authors have published related theories with massive neutrinos subject to a color SU(3) that are anomaly-free, e.g., [26] [27] [28]. The results here may be viewed as representative of a minimal neutrino SU(3) for these other extensions.

Section 2 computes cross-sections of interactions of such dark matter with conventional matter in the modern universe. Section 3 applies the hypothesis to neutrinos in the early universe, addressing the details of evolution of such matter, its free-streaming scale, and ultimate abundance. Section 4 addresses the impact on nucleosynthesis. Section 5 checks the hypothesis against SN1987a

measurements. Section 6 compares predictions with observational inferences from the cosmic microwave background (CMB). Sections 7 and 8 discuss and summarize the overall findings of this effort.

2. Cross-Sections between Ordinary Matter & Baryonic Neutrinos

The hypothesis of a feeble form of SU(3) for neutrinos is not immediately obvious from the Standard Model. From the Standard Model one might expect an interaction energy of the order of the QCD energy scale, ~200 MeV [29]. However, motivation can be found for a feeble SU(3) interaction between neutrinos in a modest extension of the Standard Model [24]. In this extension, SU(3) is not precluded for the neutrino family, and the interaction strength is related to the mass of the most massive fermion of the family, as discussed in the **Appendix**. In this theory, neutrino oscillations are direct evidence that neutrinos form bound states via SU(3).

The cross-section σ_j for neutrino scattering via $SU(3)_{\upsilon e}$, *i.e.*, "neutrino jets", is of the form

$$\sigma_{\nu j} = f\left(4\pi/3\right)\alpha^2\left(\hbar c\right)^2/s\,, \tag{1}$$

by analogy with that for quark jets [30], where the dimensionless coupling $\alpha = g^2/(4\pi\hbar c)$ is set to the fine structure constant, 1/137, s is the usual square of the center-of-mass energy of the incident neutrinos, and f scales the interaction strength from 0 to 1 or greater. Note that the $1/s$ dependence implies that the cross-section is weak at high energies, and much larger at lower energies. This behavior is in contrast with the scaling of cross-sections for electroweak interactions, such as $e^+e^- \leftrightarrow \upsilon_e\bar{\upsilon}_e$, which scale as $G_{F0}^2 s$ at the energies of interest (<3 GeV), where $G_{F0} = G_F/(\hbar c)^3$ is equal to 1.16×10^{-5} GeV^{-2} (e.g., [4], page 152).

One may simply choose f for a feeble form of SU(3) for neutrinos, or one may estimate it using $SU(3)_{\upsilon e}$. An estimate is developed in the **Appendix** using the latter approach. One finds a reduction in the coupling strength relative to quarks by a factor of $(m_\upsilon/m_b)^2$ to $(m_\upsilon/m_t)^2$ for relativistic interactions, where m_υ is the mass of the massive neutrino, and m_b and m_t are the bottom and top quark masses, respectively. Using the masses from the Particle Data Group [31] [32], m_b is about 4.180 GeV/c^2 using the minimal subtraction scheme and m_t is about 172.9 GeV/c^2 from direct measurements. The highest neutrino mass is about 0.055 eV/c^2, assuming the normal hierarchy and minimal masses [33]. With this one estimates a range for f from 3.3×10^{-18} down to 1.9×10^{-21}, accounting for the factor of 137^2 in the definition given above. In this paragraph and the rest of the paper, the specific masses of the three mass eigenstates of neutrinos will be referred to as the lowest, middle, and highest neutrino mass.

Cross-sections for neutrinos and baryonic neutrinos ("B-Neutrinos") with other forms of matter are estimated below in **Table 1**, along with the corresponding estimated interaction times in **Table 2**. The interaction times, *i.e.*, time between scattering events, denoted by τ_{int}, are estimated using the usual relation,

Table 1. Estimated cross sections (σ, barns) for solar neutrinos and baryonic neutrinos.

Neutrinos vs	Quarks	Electrons	Neutrinos	B-Neutrinos
Electroweak	0	3.0×10^{-20}	9.4×10^{-21}	4.2×10^{-27}
$SU(3)_v$	$<5.1 \times 10^{-22}$	0	2.4×10^{-19}	5.4×10^{-13}
B-Neutrinos vs	Quarks	Electrons	Neutrinos	B-Neutrinos
Electroweak	0	1.4×10^{-20}	4.2×10^{-27}	2.2×10^{-33}
$SU(3)_v$	$<2.0 \times 10^{-21}$	0	5.4×10^{-13}	9.7×10^{-7}

Table 2. Estimated interaction time at earth (years).

B-Neutrinos vs	Quarks	Electrons	Solar Neutrinos	B-Neutrinos
Electroweak	∞	2.6×10^{19}	1.7×10^{23}	1.1×10^{30}
$SU(3)_v$	$>3.6 \times 10^{17}$	∞	1.3×10^{9}	2420

$$\tau_{int} = \left(N\sigma v\right)^{-1}, \tag{2}$$

where N is the density of baryonic neutrinos, σ is the interaction cross-section, and v is the velocity of the interacting particle. N is chosen to equal $3 \times 5 \times 10^8$ cm^{-3} for matter near earth in the modern universe, based on computations provided in a companion paper [23]. The factor of 3 arises because there are 3 neutrinos per baryonic neutrino. The calculation of σ and v are detailed in the following paragraph.

To compute the cross-section, the factor f is assumed equal to 5×10^{-19}, a value comfortably within the range identified in the previous paragraphs. The parameters assumed in the calculations for Table 1 are that electrons in stellar cores have a kinetic energy of 1000 eV, solar neutrinos have a kinetic energy of 0.3 MeV, baryonic neutrinos have a kinetic energy of 0.078 eV from the **Appendix**, and quarks in baryons have a kinetic energy of 100 MeV. The computations of center-of-mass (CM) energy assume the velocities of the respective particles are perpendicular in the earth's reference frame. For comparison, results are also included for the electroweak interaction.

Table 2 emphasizes that (a) the electroweak interactions of baryonic neutrinos with ordinary matter are quite small, and (b) that $SU(3)_v$ interactions with ordinary matter are unlikely to be experimentally accessible. The interaction time with a quark is estimated at about 25 million times the age of the universe. With large quantities of quarks, many kg, an interaction might occur in a reasonable time. However, such interaction energies would be of the order of an eV, and so would be quite small compared to quark-quark interaction energies, of the order of 100 MeV or more, so might be difficult to detect. It should be noted that the estimated interaction time with a solar neutrino is about 1.3 billion years. This scattering time implies a very small probability of scattering of a solar neutrino in the 8 minutes required to travel from the sun to the earth. Also, note that the estimated scattering time between two baryonic neutrinos is relatively small, and this is consistent with a picture in which baryonic neutrinos are

weakly bound.

One might imagine that neutrinos might interact with quarks via $SU(3)_{ve}$ as indicated above by simple application of the formulae. However, as is well known, the coupling constant must be the same for the fermion-boson interaction and the boson-boson interaction for a non-Abelian local gauge interaction [[34], Ch. 16]. Given the vast estimated difference in coupling constants between $SU(3)_v$ and the standard SU(3), one is then tempted to conclude that the posited neutrino $SU(3)_v$ is a force that is distinct from quark SU(3), in which case the interaction is forbidden by gauge symmetry. However, the calculations of the **Appendix** for neutrino SU(3) interaction strengths assume the same (running) coupling parameter as in quark SU(3). Hence it is possible that neutrinos might interact with quarks via a very feeble form of SU(3). Such feeble interactions would likely by experimentally unobservable, with relative interaction strengths f that are at least 10^{17} times smaller than that between quarks.

To summarize, the hypothesized $SU(3)_v$ interaction has a coupling constant that is at least $f^{1/4} = 4.5$ orders of magnitude smaller than that of SU(3), based on the calculations of the **Appendix**. This process should also produce neutrino-antineutrino pairs (neutrino jets). All interactions with ordinary matter occur on time scales that are of the order of the age of the universe or greater. SU(3) interactions between neutrinos and quarks are evidently either forbidden by local gauge symmetry or are not experimentally observable.

3. $SU(3)_v$ Applied to Neutrinos in the Early Universe

The analysis starts by using the approach of [35], for example. The fraction of energy in the neutrino sector for $kT \approx 1$ MeV is given in **Table 3**, assuming both variants of $SU(3)_v$. Note that in this energy range, all the quarks as well as the W and Z vector bosons have frozen out and (mostly) annihilated. The table assumes the standard treatment for electron and photons. The 3 flavors of neutrinos are only given 1 spin degree of freedom, in accord with convention, but with 3 color degrees of freedom. The degrees of freedom of fermions are of course

Table 3. Energy density degrees of freedom in the early universe with kT at ~1 MeV assuming both the standard SU(3) for neutrinos, $SU(3)_{vs}$, and an extended version, $SU(3)_{ve}$.

Particle	Degrees of Freedom, $SU(3)_{vs}$	Degrees of Freedom, $SU(3)_{ve}$
Electron family	(1)(4) = 4 (×7/8)	(1)(4) = 4 (×7/8)
Photons	2	2
Neutrino family	(3)(2)(3) = 18 (×7/8)	(3)(2)(3) = 18 (×7/8)
Neutrino family gluons	(8)(2) = 16	(15)(3) + (8)(2) = 61
Total degrees of freedom	37.25	82.25
Total degrees of freedom in neutrino sector	31.75	76.75
% Degrees of freedom in neutrino sector	85.2%	93.3 %

weighted by 7/8 [[4], p. 151] for energy density calculations.

Of significance for $SU(3)_v$ is that 8 massless gluons are counted for their thermodynamic degrees of freedom. For $SU(3)_{ve}$ there are also 15 massive neutrino gluons that result from the spontaneous symmetry breaking of the nearly-exact global continuous SU(3) color symmetry that occurs in this theory. These gluons satisfy most of the criteria proposed by [36] for a correction to the observed effective number of neutrinos. In this case, such neutrino gluons may add degrees of freedom, but they will be lost as they combine with neutrinos to form dark matter. **Table 3** indicates that the fractional number of degrees of freedom in the neutrino sector is 85.2% for $SU(3)_{vs}$ and 93.3 % for $SU(3)_{ve}$ in this assumed interval of time in the early universe. These values should be compared with the currently accepted value for the DM matter fraction in the modern era of about 82% - 84% from recent PDG publications [37]. A more detailed calculation in this section will predict a value of 83%. These calculations show that the $SU(3)_v$ model provides enough degrees of freedom to account for the inferred fraction of DM.

Table 3 shows 18 neutrino-family states for both versions of $SU(3)_v$, comprising 9 neutrino states and 9 antineutrino states. There are only 18 states because all neutrinos have only one handedness rather than two as occurs for quarks, so the effective number of states is divided by 2 (there are no left-handed antineutrinos or right-handed neutrinos). This gives 18 states compared to (3)(2)(2) = 12 states assumed in published single-color calculations. This large number of neutrino states seems to be inconsistent with accelerator observations of the Z^0 linewidth, which only indicates 3 neutrino states instead of 9. The most straightforward approach for avoiding this inconsistency is to assume that neutrinos are color singlets as they pertain to the electroweak sector [[25], Ch. 13]. This is supported by the corresponding analysis for the charged-current portion of the electroweak Lagrangian density. Then the resulting contribution to the Z^0 linewidth is identical to that in the SM. This result is *not* consistent with the model-independent linewidth measurement of 2.74 ± 0.1 GeV [[38], Sec. 1.5]. This conclusion accounts for QED and QCD corrections to the individual fermion decay rates but excludes QED photonic corrections to the Z^0 lineshape. A few other independent measurements also support the larger linewidth [39]. However, if the QED photonic corrections to the Z^0 lineshape are included, the result is precisely consistent with the more-accepted value of 2.984 ± 0.008, as can be seen from the Schael reference [38] and others.

The process of particle formation and cooling with $SU(3)_v$ in the neutrino family should be analogous to that in the quark sector, but with a few important exceptions. Before neutrino decoupling, the ultra-relativistic particles are kept from particle formation by the standard electroweak interactions. Under the hypothesis of this paper, after neutrino decoupling one expects a period of intense particle formation as relativistic neutrinos collide and interact via $SU(3)_v$ resulting in neutrino-antineutrino pairs from "jets". This process is both spon-

taneous and irreversible and so results in an increase in entropy. Many hundreds of species then form during "hadronization" to bound baryonic and mesonic species, as with the quark transition [35]. This implies that there is substantial cooling as the available energy is shared among more relativistic species. If there are insufficient neutrinos remaining after this conversion (as is indeed found to be the case below), there is insufficient thermal energy to restore the hadronic neutrinos to a higher temperature. These multiple species then cool further in accord with the expansion of the universe, with $T \sim a^{-1}$ during the radiation era, with a denoting the cosmological scale factor. Since neutrinos have no means for annihilation in the Standard Model or in the extended-color theory considered here, they will not re-heat due to any annihilation process. Moreover, their free-streaming will be inhibited by the SU(3) interaction. The baryonic neutrinos will cool until they reach an energy at which they can bind, also by analogy with the quark sector. Once they have bound, they form "clumps" of inert dark matter with little diffusion or mass transport. One would then expect that further cooling occurs due to expansion of the universe over the subsequent 13.7 billion years to the present date. The above process is detailed quantitatively in the rest of this section.

Figure 1 shows the estimated time to complete a specified number of SU(3) interactions for one neutrino. The calculations use the cross-section from Equation (1) and the high levels of neutrino densities that occur at and after neutrino decoupling in Equation (2). This figure shows results for both the standard cosmology as well as with the extra degrees of freedom associated with this hypothesis. The curves show longer times with the extra degrees of freedom because

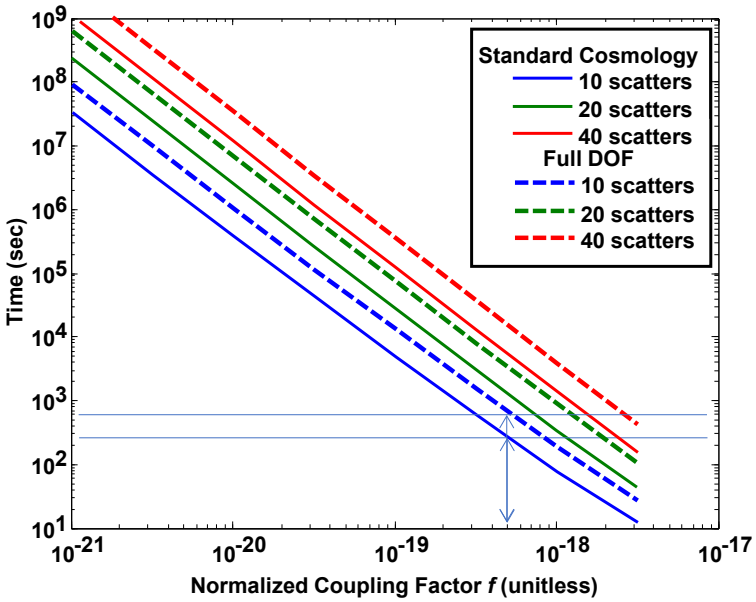

Figure 1. Time required to produce 10, 20, and 40 collisions after neutrino decoupling, versus normalized $SU(3)_v$ coupling factor, f. Solid lines: standard cosmology for temperature. Dashed lines: full degrees of freedom (second column of Table 3) used to compute temperature.

the scattering time (mean free time) given by Equation (2) is longer with extra degrees of freedom. This follows because the universe is expanding and cooling faster, resulting in lower density at a given time, so $(N\sigma v)^{-1}$ is longer. The particle density varies in time as $T^3 \sim a^{-3}$ and the velocity of all such neutrinos remain at approximately c in the interval of time shown in Figure 1. The number of interactions shown in Figure 1 can be used to compute the number of particles, also by analogy with the quark sector, in which each relativistic collision produces at least 2 particles. Hence 10 collisions will produce of the order of 2^{10} neutrino-antineutrino pairs. The calculation assumes that there are initially 18 neutrino species, consistent with Table 3, so there are 18 times more interactions that produce hadronized neutrinos. One sees that a nominal value of $f = 5 \times 10^{-19}$ results in 10 collisions in about 250 sec with the standard cosmology, and in about 600 sec with the full degrees of freedom arising from this hypothesis. It should be mentioned that the onset of this process might start with just one collision, which occurs at about 6 sec after decoupling for $f = 5 \times 10^{-19}$ and at about 30 sec after decoupling for $f = 1 \times 10^{-19}$. The calculation neglects the doubling of the density of neutrino-derivative states with each collision and the corresponding halving of temperature. If these effects are included, the time to 10 collisions is about 9 sec with the added degrees of freedom rather than 600 sec.

Regarding the types of baryonic neutrinos, there are 3 basic types of neutrinos, so there are expected to be at most $3^3 = 27$ possible basic types of a colorless baryonic triplet, just as with the discrete SU(3) symmetry for (u, d, s) states in the quark sector. There are an additional equal number of antiparticle states, and possibly 2 spin states would occur for nonrelativistic baryonic neutrinos. This leads to at most 54 species with 108 distinct baryonic neutrino states. There could also be as many as 12 distinct species for mesonic neutrino states. There are also many excited states of the basic species. Based on a study of hadrons [35], there are 1776 distinct quark states listed in the 2016 PDG publication, including charm and bottom states. If the charm and bottom states are excluded, so that only 3 basic flavors are present, as is the case here, then 1599 states are found. This is the number used here for the number of species, g_{bv}, of baryonic and mesonic neutrinos in the early universe after $SU(3)_\nu$ conversion. This number should be viewed as approximate, but perhaps conservative because other species such as baryonic neutrino "nuclei" may be present.

With the results of Figure 1 and an estimate for the number of post-conversion species of hadronic neutrinos from the previous paragraph, one can compute the temperature after conversion to baryonic neutrinos. Conservation of energy of course applies in this process. Conservation of energy gives

$$g_{vd}\rho_{vd}T_{vd}a_{vd}^4 = g_{bv}\rho_{bv}T_{bv}a_{bv}^4, \tag{3}$$

where g_{vd}, ρ_{vd}, T_{vd}, and a_{vd} are the number of species, number density of each species, temperature, and scale factor at neutrino decoupling, respectively. The variables with subscript "bv" are the corresponding variables just after conversion to hadronic neutrinos. The increase of entropy during the conversion process

gives the inequality [4] [35]

$$g_{vd}\rho_{vd}a_{vd}^3 \ll g_{bv}\rho_{bv}a_{bv}^3, \tag{4}$$

where $\rho \sim T^3$ is used in this relativistic era. From Equation (4), the ratio of the comoving density at decoupling to the density after conversion, per species, satisfies

$$\rho_{vd}a_{vd}^3/\left(\rho_{bv}a_{bv}^3\right) \ll g_{bv}/g_{vd}\ . \tag{5}$$

The number of degrees of freedom for energy density in the neutrino sector at decoupling, denoted g_{vd}, is 76.75 from **Table 3** for the extended-color version. Of these, one should exclude the degrees of freedom of conventional neutrinos, which numbers 6(7/8) = 5.25 resulting in $g'_{vd} = 71.5$ species. The number of degrees of freedom after conversion is g_{bv} = 1599, as given above. Hence Equation (5) implies that the ratio of the number of particles per species in a comoving volume before and after conversion should be less than 1559/71.5 = 21.8 from Equation (5). If the standard-model version is used from **Table 3**, this ratio is 1599/26.5 = 60.3. If the number of states is divided by 2 for neutrino-based particles because of their handedness, this ratio is 799/26.5 = 30.2. Given that relativistic collisions produce hundreds of particles in observed accelerator collisions of protons, and relativistic collision products should equilibrate rapidly in this dense relativistic environment, with energy-level separations ΔE much less than kT, one finds

$$\rho_{vd}a_{vd}^3/\left(\rho_{bv}a_{bv}^3\right) \approx 1\ . \tag{6}$$

That is, the number of particles of each resultant species in a comoving volume should be approximately equal to the number of original particles of each species in the volume (as one might expect). Using this as an exact equality in Equation (3) gives

$$T_{bv}/T_{vd} < \left(g_{vd}/g_{bv}\right)\left(a_{vd}/a_{bv}\right) = \left(1/21.8\right)\left(a_{vd}/a_{bv}\right), \tag{7}$$

assuming $SU(3)_{ve}$. That is, the temperature of hadronic neutrinos after conversion should be about 1/21.8 = 4.6% of what it would be for neutrinos in the absence of conversion. To complete the computation of T_{bv}/T_{vd}, one may for example use the ~250 sec highlighted in **Figure 1** for the standard cosmology. One may also use a temperature at neutrino decoupling of 0.83 MeV/k [40] [41] [42], and a proportional to time$^{1/2}$ during this era. With these inputs, one obtains an estimate of the average temperature of a hadronic neutrino species after conversion:

$$T_{bv0} \le 2.4\ \text{keV/k}\ . \tag{8}$$

This result assumes $SU(3)_{ve}$. The result for $SU(3)_{vs}$ is 1.7 keV/k using the ratio 30.2 given above. In addition, each particle so created has a mass of the order of 0.4 eV/c^2 based on the calculation of the **Appendix** and [23], which is about a factor 17 greater mass than the average mass of the three neutrino species (0.07/3 = 0.0233 eV/c^2, 0.4/0.0233~17). It should be noted that T_{bv0} will be less when the full number of neutrino degrees of freedom are included in the calculation of

temperature versus time and time versus scale factor (Equation (9) below). When this is done, the value of T_{bv0} in Equation (8) is reduced to about 1.7 keV/k, and this includes the impact of a slightly larger value of a_{vd} as well as a slightly reduced temperature at neutrino decoupling.

It should be further noted that with about 71.5 original degrees of freedom for hadronic neutrinos but only 5.25 degrees of freedom for conventional neutrinos, the remaining degrees of freedom of conventional neutrinos are almost certainly insufficient to appreciably heat the hadronic neutrinos, despite that they should be well-coupled. Hence the temperature given by Equation (8) remains a good approximation in the presence of neutrinos that might be hotter.

The evolution of the temperature and state of the baryonic neutrinos is now discussed. The basic equation for time t after infinite redshift versus the normalized scale factor a is given by, e.g., [[43], Ch. 13]

$$t(a) = H_0^{-1} \int_0^a \mathrm{d}x \left[\Omega_r(x) x^{-2} + \Omega_m(x) x^{-1} + \Omega_k + \Omega_\Lambda x^2 \right]^{-1/2}. \quad (9)$$

In standard cosmology, Ω_r, Ω_m, and Ω_Λ are constants after neutrino decoupling, and are the radiation energy density, matter energy density, and dark energy density ratios, respectively, of the universe. Ω_k represents contribution of the curvature constant. The value used for the present-day Hubble expansion rate H_0 is 67.8 km sec^{-1} Mpc^{-1} [37]. The standard constant values for Ω_r and Ω_m are most accurately provided from the Planck collaboration [44] [45]. In the treatment here, Ω_m and Ω_r will vary with time until the hadronic neutrinos become nonrelativistic:

$$\Omega_m(x) = \begin{cases} \Omega_{m0} = 0.05 & \text{for } x < x_{non-rel} \\ \Omega_{m1} = 0.31 & \text{for } x > x_{non-rel} \end{cases}, \text{ and} \quad (10a)$$

$$\Omega_r(x) = \begin{cases} \Omega_{r0} = F 9.13 \times 10^{-5} & \text{for } x < x_{non-rel} \\ \Omega_{r1} = 9.13 \times 10^{-5} & \text{for } x > x_{non-rel} \end{cases}. \quad (10b)$$

The factor F in Equation (10b) is numerically equal to 6.52 and is based on the number of degrees of freedom in the second column of **Table 3**, relative to the standard number of degrees of freedom:

$$F = \left\{ 1 + \left[(16+45)/2 + (18/2)(7/8) \right] (4/11)^{4/3} \right\} \Big/ \left[1 + 3(7/8)(4/11)^{4/3} \right]. \quad (11)$$

The value of $F^{1/4}$ is about 1.60, which gives the scaling for time and temperature as detailed below. The integral in Equation (9) is performed with this variation included, as well as with the standard and fixed values of Ω_m and Ω_r as given in Equation (10) after neutrino decoupling. The neutrino sector temperature is then computed versus time using $T_{bv}(t) = T_{bv} a_{bv} / a(t)$. The result is shown in **Figure 2**. This figure shows a constant-factor drop in temperature at early times when the full number of degrees of freedom are used in Equation (9) relative to standard cosmology. This is expected because $T \propto a^{-1} \propto \Omega_r^{-1/4} t^{-1/2}$ in the radiation dominated era, and with a larger value of Ω_r, the full 82.25 degrees of freedom of **Table 3**, the temperature is reduced by about a factor $F^{1/4}$ of 1.6 as noted

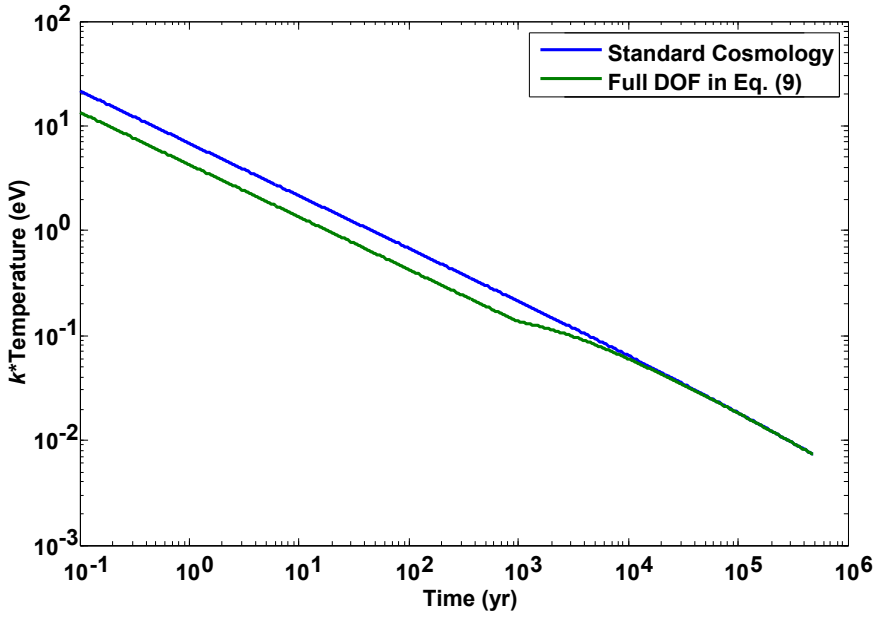

Figure 2. k^* Temperature (eV) of free baryonic neutrinos versus time (yrs), assuming conversion at 250 sec, for standard cosmology (blue) with Ω_m and Ω_r at their standard and fixed values, and with the time-varying values given by Equation (10) (green).

above. An investigation of the underlying numbers in Figure 2 shows that the time to recombination is altered down from its nominal value of about 380 kyr by about 0.4% due to the extra degrees of freedom. This figure shows that the additional relativistic degrees of freedom in the neutrino sector at early times does not appreciably alter the time history after about 3000 years, because such degrees of freedom convert to nonrelativistic matter very early, at about 1100 years after neutrino decoupling or less using the standard criteria, $kT = m_{bv}c^2/3$ (1100 years for $m_{bv}c^2$ = 0.4 eV, 435 years for $m_{bv}c^2$ = 0.6 eV). This can be seen from Figure 2. The apparent convergence of the two curves after about 2000 years occurs because of the log-log plot and the relatively diminishing contribution of the early-time integral at later times. Also, the crossover from radiation-dominated to matter-dominated expansion occurs at about 50 kyr but this is difficult to discern on this plot.

Next, neutrino streaming is investigated. The standard formula for the free streaming length λ_{fs} is [46] [47]

$$\lambda_{fs} = \int_{t_0}^{t_{eq}} v(t)/a(t)\,\mathrm{d}t\,, \tag{12}$$

where t_0 in this case is the time of neutrino decoupling, t_{eq} is the time of matter-radiation equality at about 50 kyr after infinite redshift, $v(t)$ is the particle velocity versus time, and $a(t)$ is the scale factor versus time. The velocity of the neutrinos before hadronic conversion is c.

The velocity will also be c after conversion (at time t_{conv}) until the time t_{nr} at which $<K.E.>/m_{bv}c^2$ is roughly equal to 1/3, where $<K.E.>$ denotes the mean kinetic energy, in accord with the standard criterion. Then the velocity will be

nonrelativistic until such time when $<K.E.>/E_{bind}$ is equal to 1, where $E_{bind} \sim 0.02$ eV, at which point macroscopic binding occurs and little motion occurs thereafter [23]. The above three regimes are all captured accurately in a numerical integral of Equation (12), where the integral is extended beyond t_{eq} to the time of neutrino binding, t_{bind}, as needed. The result of the numerical integral for a particle mass $m_{b\nu}c^2$ of 0.4 eV is a free-streaming scale length of about 90 Mpc, using the peculiar velocity for v after particles become nonrelativistic. This is significantly less than the zeroth-order estimate of $41(30/m_{b\nu}c^2$ eV) = 3075 Mpc computed by others [48] [49] because of the factor of 22 temperature drop at conversion. However, 90 Mpc is still quite large compared to galactic scale sizes, assuming ballistic motion.

The above calculation is for ballistic motion of neutrinos or baryonic neutrinos, and this would be expected to apply prior to conversion to baryonic neutrinos. However, the likely form of motion is diffusive rather than ballistic after conversion. After conversion there are approximately 1600 species of baryonic and/or mesonic neutrinos und this hypothesis, which are densely packed and all can interact with each other via $SU(3)_\nu$. The corresponding mean free time between collisions can be computed via Equation (2), with an extra factor of 1600 included in the density. The resulting mean free time is quite short. For example, just after conversion, at 200 sec after neutrino decoupling and with $m_{b\nu}c^2 = 0.4$ eV, the mean free time between collisions is about 130 sec using Equation (2) and the associated cross-sections. Alternatively, if the particles interact like hard spheres (consistent with other forms of matter bound by SU(3)), then the mean free time between collisions is given by

$$t_{int} = \left(2^{1/2}\pi g_{b\nu} N d^2 v\right)^{-1}, \tag{13}$$

where $g_{b\nu}$ is given after Equation (5) and d is the particle "radius". In this case of a degenerate Fermi fluid, the radius can be set to $\hbar/p_F$, where p_F is the Fermi momentum of the particle. The resulting mean free path is about 137 fm, and the mean free time is about 4.4×10^{-22} sec, an astonishing result. Because the longer interaction times from Equation (2) are consistent with a more tenuous medium, it will be referred to as a "gaseous" case, whereas the case corresponding to Equation (13) will be referred to as a "fluid." Both of these mean free times (gas or fluid) are much shorter than the overall times of interest, $t_{nr} - t_0$ and $t_{eq} - t_0$, which are of the order thousands of years or more. It should be noted that a more complete and correct computation of cross-sections for fermion gases can be found in the literature, e.g., for neutrinos in supernovae [50], and would likely involve partial blocking to final states that follow from the Pauli exclusion principle [51]. Calculation of these nine-fold integrals is beyond the scope of this paper. A simplified calculation involving one-dimensional integrals [[4], p. 161] gives about a 35% increase in scattering times. In any event, the transport evidently should be considered diffusive rather than ballistic. Hence Equation (12) can be reformulated using

$$\left\langle \boldsymbol{v}(t_1)\cdot\boldsymbol{v}(t_2)\right\rangle = \kappa(t_1)\delta(t_1-t_2), \tag{14}$$

which results in a root-mean-square (RMS) streaming scale given by

$$\left\langle \left|\boldsymbol{\lambda}_s\right|^2\right\rangle^{1/2} = \left[\int_{t_0}^{t_{bind}} \kappa(t)/a^2(t)\,\mathrm{d}t\right]^{1/2}. \tag{15}$$

Note in the above that κ has units of m^2/sec, and such a diffusivity can be estimated from $\kappa(t) = v(t)^2\,\tau_{int}(t)$ after conversion ($\tau_{int}(t)$ is given by Equation (2)). The ballistic calculation still applies before conversion to baryonic neutrinos, at least to a first approximation.

Table 4 shows the result of the above calculations for both gaseous and fluid states of matter using a conversion time of 200 sec (a bit before the posited nominal time to complete conversion), for a range of baryonic neutrino masses. The calculation of the RMS streaming length is based on Equation (15) and is done using two different approaches. The first approach is based on the standard scaling of conformal (peculiar) velocity with a^{-1} after the particle velocity drops slightly below c. The second approach uses the RMS velocity v_{rms}, which is obtained by solving $\langle K.E.\rangle = m_{bv}c^2\left\{\left[1-\left(v_{rms}/c\right)^2\right]^{1/2}-1\right\}$. This latter approach may be applicable when the velocity is randomly varying over time.

An analysis of the contributions to the streaming length indicates that almost all of the particle motion occurs before hadronic conversion for the case of a liquid state of baryonic matter, whereas almost all the particle motion occurs after conversion for a gaseous state.

The former is because there is essentially no particle motion after conversion for a liquid state. There is also no mass dependence for the fluid state because all particles move at velocity c before conversion. It is of particular interest to note that the RMS streaming length for the liquid state is about 0.84 kpc, and for the gaseous state it is less than about 180 kpc for a baryonic neutrino with a mass in the vicinity of 0.4 eV/c^2. These numbers bracket the range of what one might expect for an early galactic halo that evolves little after initial formation. The numbers of Table 4 are 65% to 94% smaller than one would obtain if one used the standard cosmology with Ω_m and Ω_r fixed at their standard values. This is due to the fact that $a^{-1} \sim \Omega_r^{-1/4}$ and with Ω_r larger with more degrees of freedom, a^{-1} is smaller, so the integrals in Equation (15) are numerically smaller.

The above calculations are all for a representative conversion time of 200 sec. However, this time was simply a choice consistent with Figure 1, and not derived. To address this, the sensitivity of key calculated parameters to this choice

Table 4. RMS streaming length λ_s (kpc) versus particle mass (eV/c^2) from Equation (15), assuming a conversion time of 200 sec and full degrees of freedom in Equation (9).

	$m_{bv}c^2$ = 0.2 eV/c^2	0.4	0.8	1.2	1.6
λ_s (fluid)	0.836	0.836	0.836	0.836	0.836
λ_s (gas, v from a^{-1})	147	114	85.1	71.9	63.5
λ_s (gas, v from K.E.)	177	157	137	125	118

of conversion time is shown in Table 5. A particle of mass 0.4 eV/c^2 is assumed in this table. This table shows that several key parameters are essentially independent of the conversion time, such as the time at which the particles becomes nonrelativistic, t_{nr}, and the time at which the particles bind, t_{bind}. This behavior is expected because the relativistic energy density is the same in all cases for these time periods. It should be noted that the time to macroscopic binding, t_{bind}, is not sensitive to t_{conv}, but it is sensitive to the energy of binding. For example, if the binding energy is changed from 0.02 eV to 0.01 eV, the estimated time of binding changes from 85 kyr to 285 kyr from Figure 2. The RMS streaming lengths show some variation, particularly for the liquid phase. This variation for the liquid phase is expected based on the discussion above, because all the streaming occurs in the time before conversion of free neutrinos to hadronic neutrinos in this case, and this time interval is explicitly varied.

One might also consider the sensitivity of the streaming length to the number of degrees of freedom, post-conversion. Based on the above, there is essentially no variation of the streaming length with g_{bv} for the case of a diffusive liquid. For the case of a diffusive gas, it is easy to see from Equation (2) with a factor of g_{bv} in the denominator and using Equation (15) that λ_s scales as $g_{bv}^{-1/2}$. So, for example, if the number of degrees of freedom drops by a factor of 2 between conversion and t_{nr}, perhaps due to decay of excited states, then the streaming length will go up by a factor of $2^{1/2}$ for the case of a diffusive gas. However, there is no clear way to compute the decay times of such excited states so it is not included in the calculations.

The number of effective degrees of freedom in the neutrino sector, N_{eff}, can be estimated from the above. First, from Table 3, second column, there are 71.25/2 × (8/7) = 40.8 extra relativistic generations of neutrinos compared to the 3 generations in the conventional neutrino sector. Second, from the preceding discussion these extra relativistic degrees of freedom persist for about t_{nr} = 1100 years over the total time of about 380,000 years to recombination. Thus, one can estimate the correction to N_{eff} to be in the range of 40.8 × (1100/3.8 × 10^5) = 0.118. If a mass of 0.6 eV/c^2 is relevant, then t_{nr} = 480 years, and the correction to N_{eff} is then 0.047. It should be mentioned that there are as many as 1600/2 relativistic (but cooler) "generations" relative to photons after conversion, as discussed above, but the relativistic comoving energy density is conserved through conversion in accord with Equation (3). Hence the 40.8 generations is an upper bound to properly capture the number of relativistic degrees of freedom relative

Table 5. Key calculated parameters as a function of conversion time, t_{conv}. Assumes a baryonic neutrino mass is 0.4 eV/c^2, assuming full degrees of freedom in Equation (9).

t_{conv} (sec)	kT_{conv} (keV)	t_{nr} (yrs)	t_{bind} (yrs)	$\lambda_{s,gas,rms}$ (kpc)	$\lambda_{s,fluid,rms}$ (kpc)
20	5.5	≤1100	8.45×10^4	112.9	0.26
200	1.70	≤1100	8.45×10^4	113.5	0.84
2000	0.550	≤1100	8.45×10^4	115.3	2.65

to photons. This range of values of correction to N_{eff} (0.047 to 0.118) overlaps with most observational estimates [37] [44] [45]. This also in part confirms the speculation in [36] that the oft-observed excess of N_{eff} over 3 can be explained by the use of Goldstone bosons from the spontaneous symmetry breaking of an exact or nearly exact global continuous symmetry (which is indeed the case in the context of this hypothesis).

One implication of the early conversion, cooling, diffusive transport, and binding of such baryonic neutrinos is that their signature is one of relatively heavy particles. From this, it follows that such matter would behave in a similar manner to that of cold dark matter with respect to baryon acoustic oscillations (BAOs) at the time of recombination, so it is unlikely to be discernably different from the conventional analysis of the BAO spectrum. This qualitative statement should be backed up by more detailed calculations; these are not performed here.

At the aforementioned time of binding of such baryonic neutrinos, ~85 kyr, such particles should begin to coalesce into distinct bodies. One may then consider the possibility of pressure equilibrium between such bodies of baryonic neutrinos and surrounding free neutrinos. Assume in this case that the highest-mass neutrino (denoted τ, assuming the normal hierarchy) is not relativistic and the lower mass states are still marginally relativistic. Further, for simplicity, assume that there are only two species of baryonic neutrinos that remain (*i.e.*, particle and antiparticle). In this case, one obtains the following relationship for pressure equilibrium:

$$\left(1.914\hbar^2/m_{b\nu}\right)\rho_{b\nu}^{5/3} = \left(1.914\hbar^2/m_{\nu\tau}\right)\rho_{\nu\tau}^{5/3} + 5.536\hbar c\rho_{\nu\mu}^{4/3} + 5.536\hbar c\rho_{\nu e}^{4/3}. \quad (16)$$

Here $m_{\nu\tau}$ and $\rho_{\nu\tau}$ denote the mass and number density of the highest-mass neutrino state, respectively. Assuming that the neutrino-state densities are all comparable and equal to ρ_ν, one obtains

$$\rho_{\beta\nu}/\rho_\nu = \left[\left(m_{b\nu}/m_{\nu\tau}\right) + (2)5.536m_{b\nu}c^2/\left(1.914\hbar c\right)\rho_\nu^{-1/3}\right]^{3/5}. \quad (17)$$

One may evaluate Equation (17) for an assumed mass of a baryonic neutrino of about 0.4 eV/c^2, and the assumed masses of the neutrinos as given in the **Appendix**. The result is shown in **Table 6** as a function of temperature, with the hypothesis of equilibrium.

One sees that for temperatures less than 0.03 eV/k, which are consistent with a kinetic energy of the order of $2m_{\mu\nu}c^2$, one obtains a number density ratio ranging

Table 6. Number density ratio and mass density ratio of baryonic and conventional neutrinos, assuming $m_{b\nu} = 0.4$ eV/c^2 and $m_{\tau\nu} = 0.055$ eV/c^2 in Equation (17).

kT (eV)	0.1	0.07	0.03	0.02	0.01
$\rho_{e\nu}$ (m^{-3})	3.2×10^{16}	1.1×10^{16}	8.6×10^{14}	2.5×10^{14}	3.2×10^{13}
$\rho_{b\nu}/\rho_{e\nu}$	11.1	13.8	18.6	23.5	35.2
$m_{b\nu}\rho_{b\nu}/(\Sigma m_{i\nu}\rho_\nu)$	63.7	78.9	106	134	201

from 19 to 35. The mean value is 25.8. This range of ratios overlaps the values of g_{bv} = 21.8 for $SU(3)_{ve}$ and g_{bv} = 30 to 60 for $SU(3)_{vs}$ as discussed above. The number density ratios of 19 to 35 shown correspond to Ω_{DM}/Ω_{ν} of 106 to 201 as seen in **Table 6**, assuming roughly equal neutrino densities for the two lower-mass states as above. These mass density ratios should be applicable to the mass-energy density ratio observed today, which range from 0.26/0.016 = 16.5 to 0.258/0.0012 = 217, with a nominal value of $0.258/\Sigma_i m_{i\nu}/(93.4\text{ eV}/h^2)] = 158.2$, from the "Astrophysical Constants" numbers in a recent PDG publication [37]. Here h denotes the normalized Hubble constant and use $\Sigma_i m_{i\nu} = 0.07\text{ eV}/c^2$. The value of 158.2 for Ω_{DM}/Ω_{ν} is squarely in the range of values shown in **Table 6**. The mean of the relevant calculated values from **Table 6** is $\langle \Omega_{DM}/\Omega_{\nu} \rangle = (106+134+201)/3 = 147$, which is a fair match to the nominal observational value of 158.2. There is some sensitivity of this result to the assumed number and masses of baryonic species at this time. For example, if there is a second, heavier species of mass 0.6 eV/c^2 with an abundance equal to 25% that of the mass of 0.4 eV/c^2, the computed result would change from 147 to 160, which is in even better agreement with the nominal observational value of 158.2.

Further one may compute the normalized energy density of DM, Ω_{DM}, by multiplying the above value of $<\Omega_{DM}/\Omega_{\nu}>$ by Ω_{ν}. The nominal value of Ω_{ν} is equal to $\Sigma_i m_{i\nu}/(93.4\text{ eV } h^2) = 0.0016$, with $\Sigma_i m_{i\nu} = 0.07\text{ eV}/c^2$ as assumed in the rest of this paper. The resulting estimate for Ω_{DM} is therefore (147)(0.0016) = 0.240, which is in fair agreement with the nominal accepted value of 0.258. Finally, it follows that $\langle \Omega_{DM}/\Omega_m \rangle = 0.240/(0.240+0.0484) = 0.832$, using Ω_b = 0.0484 for baryonic matter from the 2018 PDG reference. This fraction, 83.2%, is in very good agreement with the observationally-inferred value of 84.2% from the same PDG reference. Of course, the error bars on the computed value of 83.2% are quite large based on the error bars of just the baryonic mass m_{bv} of 0.4 eV/c^2, as well as the error bars of the assumed value of the sum of the neutrino masses. One may therefore accuse the result of 83.2% versus 84.2% of being fortuitous, but it might best be interpreted as an indication of consistency of the assumed and/or estimated masses with key observationally-inferred data in the context of the hypothesis of this paper. As a final note on **Table 6**, the inferred number density of baryonic neutrinos for kT = 0.02 eV is consistent with the Fermi energy derived in [23] for the cores of modern galactic haloes.

One may estimate error bars for the above mass-energy density ratios by considering the spread of the two estimates of number density ratio obtained above in two different ways: 21.8 from counting states for $SU(3)_{ve}$ at hadronic conversion and 25.8 from pressure equilibrium. One-half the spread is an estimate of the uncertainty in the estimate, which is about 1.95. Dividing this by the mean of these two numbers gives an estimate of the relative uncertainty, 8.2%. Other contributors to the uncertainty are the masses of the neutrinos and baryonic neutrinos, which is of the order of 10% or more. The positive relative uncertainty should be no more about 93.3/83.2 − 1 = 12.1% (10.1% absolute error) based

on Table 3, which gives the maximum fraction (93.3%) of the neutrino sector's mass-energy density to the total mass energy density at decoupling. Similar error bars are obtained using a ratio of states of about 30 for $SU(3)_{vs}$ at hadronic conversion.

To summarize this section, the posited form of baryonic matter is found to become nonrelativistic at about 1100 years after neutrino decoupling from OM, so these particles fall into the category of warm dark matter (WDM). This section finds that the hypothesis of baryonic neutrinos has consistency with the gross features of cosmology that have been observationally inferred. First, good consistency is found between computed and observationally-inferred values of Ω_{DM}/Ω_{ν} (147 versus 158, respectively) and Ω_{DM}/Ω_{m} (83.2% versus 84.2%, respectively) in the modern era. Second, the primordial RMS streaming length computed here lies in the range of 0.25 kpc to about 180 kpc, from Table 4 and Table 5. Third, the scale sizes of this form of matter are not expected to evolve substantially once bound because of the long diffusion time constants over distances of the order of a kpc or more [23] and will not collapse due to fermion degeneracy pressure.

There are a number of details of early evolution which have not been addressed in this section. For example, an analysis should be performed for the time evolution of this form of DM from early bound entities to the condensed state for the modern era that is found in [23]. Concurrence with BAO measurements should be checked more carefully. The concurrence with nucleosynthesis is addressed in the next section. Overall, this section finds that most neutrinos "hadronize" in less than 300 sec after neutrino decoupling, become non-relativistic after about 1000 years, and then bind into macroscopic entities at about 85 kyr.

4. The Hypothesis and Nucleosynthesis

The number of degrees of freedom in the neutrino family is known to impact BBN observables as discussed in [41] [47] [52] [53]. The proposed new self-interaction of neutrinos does not directly change BBN. It is only the additional number of neutrino states associated with $SU(3)_{\nu}$ which changes BBN. Before proceeding it should be noted that it is undoubtedly striking to consider 18 or more degrees of freedom in the neutrino sector, when most of the BBN community are currently concerned with small differences from the nominal 6 degrees of freedom (3 generations).

Despite that, consistency with observations is shown below using *both* a modern precision program for primordial nuclear abundance as well as widely-published first-order formulae. The exception is deuterium abundance. This consistency is accomplished *solely* with the added number of neutrino states. The increased expansion rate of the universe due to added neutrino states is balanced with a justifiable temporary increase in weak interaction rates from such added electron neutrino states. Such added neutrino states then vanish as neu-

trinos "hadronize." A variant of this approach has been discussed by other authors [40].

It is worth devoting a paragraph to the history of calculations for BBN. The first key paper [54] considered only the impact of neutron beta decay for the reduction in neutrons. That paper was soon followed by [55] which identified the importance of the interconversion of neutrons and protons via interactions involving neutrinos. These papers neglected the now-known factor of one-half reduction in the number of neutrino states due to limited handedness and also used crude estimates for the weak interaction rates [53]. The first modern calculations of these rates were given by [56] and [57]. The use of BBN theory and observations to constrain the extra degrees of freedom at BBN was first performed by [58] and [59]. Good review publications of the above are [53] and [47]. Over the years other groups have refined this work, including [60] [61] [62] [63] and particularly [41].

The most central observable related to BBN is the helium mass fraction, conventionally denoted Y_p. The first-order change in Y_p due to additional neutrino generations is given by [52] [53]

$$\Delta Y_p \approx 0.013 \Delta N_\nu \tag{18}$$

where ΔN_ν is the change in the number of neutrino generations. Note that the number of neutrino generations N_ν should be related to the number of energy-density degrees of freedom (*DOF*) in the neutrino sector at early times from **Table 3** by

$$N_\nu = DOF/(7/4), \tag{19}$$

so that adding 2 new number-density neutrino degrees of freedom when multiplied by the factor to convert to energy density (7/8) results in a change in N_ν of 1. Also, the new degrees of freedom of neutrinos can contribute to an increased interaction rate Γ, and this in turn impacts helium mass abundance. The first order relation for this effect is given by [[41], Equation (7)]:

$$\Delta Y_p / Y_p = -0.73 \Delta\Gamma/\Gamma . \tag{20}$$

From the discussions surrounding **Table 3** above, the number of left-handed neutrinos for $SU(3)_{ve}$ should be triple that of the conventional theory (such added states are destined to become baryonic neutrinos). In this case, ΔΓ/Γ should therefore be 2. Combining Equations (18) and (20) one obtains

$$\Delta Y_p / Y_p = -0.73 \Delta\Gamma/\Gamma + \left(0.013/Y_p\right)\Delta N_\nu . \tag{21}$$

One may use Y_p = 0.245 from [52] on the right-hand side of Equation (21). For $SU(3)_{vs}$ one obtains N_ν = 31.75/(7/4) = 18.1 equivalent neutrino generations from Equation (19) and **Table 3**, first column. Thus, ΔN_ν is 18.1 - 3 = 15.2 for $SU(3)_{vs}$. For $SU(3)_{ve}$, from Equation (19) and **Table 3**, second column, one obtains 76.75/(7/4) = 43.8 equivalent neutrino generations. The corresponding value of ΔN_ν is 40.8. Clearly these changes in N_ν are not small, first-order changes. One may nonetheless apply formula (21) with these values of ΔN_ν. Set-

ting ΔYp to zero gives the following values for $\Delta\Gamma/\Gamma$:

$$\Delta\Gamma/\Gamma = 1.097 \quad \text{for} \quad SU(3)_{vs}, \quad \Delta\Gamma/\Gamma = 2.97 \quad \text{for} \quad SU(3)_{ve}. \tag{22}$$

These "first-order" results show that the required relative increase in reaction rates due to increased electron neutrino species, $\Delta\Gamma/\Gamma$, are in the vicinity of 2 that is expected for an $SU(3)_v$ theory.

To investigate the effect on BBN of the increased number of neutrino states and associated reaction rates more carefully, the state-of-the-art PRIMAT program is used [41]. This MATHEMATICA-based program allows for direct input of the number of neutrino generations, (e.g., 3, 18.1 and 43.8 as given above), and also allows for the modification of the weak interaction rates to account for the predicted extra electron neutrino states. The modification to these rates uses a transient increase in the weak interaction rates, $\lambda_{n\to p}$ and $\lambda_{p\to n}$. This time-dependent factor given by

$$r_{eff}(t) = \left[\Delta\Gamma\left(t = t_0\right)/\Gamma\right]\exp\left(-t/t_{conv}\right) + 1. \tag{23}$$

Note that $r_{eff}(t)$ tends to 1 when t is much greater than t_{conv}, the user-specified conversion time to hadronic neutrinos. Thus, the effective neutrino interaction rate will match that due to conventional neutrinos after non-conventional neutrinos have "hadronized." Note also that $r_{eff}(t)$ is equal to $\Delta\Gamma(t = t_0)/\Gamma + 1$ at time t_0. Here $\Delta\Gamma(t = t_0)/\Gamma$is also pre-specified by the user with this minor modification of PRIMAT. The value of t_{conv} was varied from about 7 sec to 300 sec. This range of times corresponds to the time to 1 to 10 collisions for $f \sim 5 \times 10^{-19}$, as shown in **Figure 1** and discussed in associated text. It should be noted that the time in Equation (23) is computed from $t = (0.8\ \text{MeV-sec}^{1/2}/kT)^2$, in approximate accord with the standard formula, e.g., [[42], Equation 10.18]. The value of $\Delta\Gamma(t_0)/\Gamma$ is chosen as seen in **Table 7** below to obtain $Y_p = 0.245$ in order to match observations.

Table 7. BBN abundance fractions for key nuclei and He mass abundance ratio Y_p at the end of nucleosynthesis. "N/A" denotes "not available."

Run #	N_v	$\Delta\Gamma(t_0)/\Gamma$	t_{conv}	p	Y_p	D/H(10^5)	^{3}He/H(10^5)	(^{7}Li+^{7}Be)/H(10^{10})
1	3	0	N/A	0.753	0.2471	2.4594	1.0741	5.6684
2	4	0	N/A	0.740	0.2597	2.7930	1.1200	5.1720
3	3	0.1	300	0.769	0.2313	2.3731	1.0607	5.4329
4	44	2.8	30	0.755	0.2453	10.5763	1.7850	1.2506
5	18	1.1	67	0.755	0.2453	5.7495	1.4380	1.8516
6	18	1.35	30	0.755	0.2446	5.7434	1.4365	1.8469
7	18	1.65	15	0.757	0.2432	5.7222	1.4340	1.8392
8	18	2.0	7.5	0.755	0.2449	5.7483	1.4371	1.8470
Observations (PDG 2018)				N/A	0.245 ± 0.003	2.569 ± 0.03	(*)	1.6 ± 0.3
Observations (Pitrou *et al.* 2018)				N/A	0.2449 ± 0.004	2.527 ± 0.03	<1.1 ± 0.2	1.58 ± 0.3

(*) PDG 2018 deliberately does not state a value for ^{3}He/H.

PRIMAT was first checked to ensure it matched the published results with 3 neutrino generations and no change in rates. The first-order changes, Equations (18) and (20), were also verified using the code. These are runs 1 to 3 shown in Table 7. The input value of the baryon-to-photon ratio was not altered from nominal for any of the runs of Table 7. Then cases related to the hypothesis of this paper were run and a subset of these runs is shown in Table 7. These results were spot-checked for convergence by increasing the number of time steps by a factor of 1.5. The results were the same to within 5 significant digits as those with the nominal number of time steps. The first column of the table is the run designator, the second through fourth columns are input values. Green indicates values within experimental error bars, brown-orange between 1 and 2σ, and red outside of 2σ.

Note that the abundance ^{7}Li/H in Table 7 uses (^{7}Li + ^{7}Be)/H as a proxy, in accord with the methodology of [41] and predecessor papers because of the known long duration and associated computational run-time required for ^{7}Be to convert to ^{7}Li for the latter's final abundance. For a similar reason, the contribution of tritium is included in ^{3}He/H in rows 1 to 3. The tritium contribution increases the values shown by about 1%. The error bars for the computations in Table 7 should also reflect published values computed for PRIMAT, but this has not been independently verified.

Runs 4 through 8 show good agreement with Y_p by design. It is interesting to note that these runs also show good agreement with observationally-inferred values of (^{7}Li + ^{7}Be)/H. This good agreement is *not* found in the standard cosmology. The agreement is particularly good for the cases with 18 generations, corresponding to the case of no massive gluons ($SU(3)_{vs}$). The cases with 18 generations are also within 2σ of the observational estimates for ^{3}He/H. In contrast with these agreements, the D/H values for 18 generations are about 110 standard deviations from the latest observationally-inferred values for gas-phase conditions [64], although the relative difference is a mere factor of 2.28. The case with 44 generations is in even greater disagreement. This potential inconsistency for D/H will be discussed in more detail below.

Several other useful comments can be made about the runs in Table 7. Not shown is the time to complete conversion to ^{4}He. In runs 1 through 3, the conversion to ^{4}He occurred between 200 and 300 sec, consistent with Figure 3 of [41]. For runs 5 to 8 with 18 generations, the conversion to ^{4}He occurred between roughly 130 and 190 seconds. For run 4 with 44 generations, this conversion occurred between roughly 100 and 130 sec. Faster conversion with more neutrino generations is expected because the universe expands faster and therefore cools more quickly.

There is also the question of consistency of $\Delta\Gamma(t_0)/\Gamma$ with the expected value based on the theory and the Z^0 linewidth. Run 8 has $\Delta\Gamma(t_0)/\Gamma$ exactly equal to 2 to match the measured He abundance and also matches the measured Z^0 linewidth as discussed above.

For run 4 with 44 generations, the value of $\Delta\Gamma(t_0)/\Gamma$ is 2.8, which is in good qualitative agreement with the predicted value of 2.97 from Equation (22). This value is required to match the measured He abundance and is significantly greater than the predicted value of 2 from quantum field theory. Hence this value is not immediately consistent with the extended-color version of SU(3) for neutrinos and with Z^0 linewidth measurements. The most straightforward means for avoiding this inconsistency is to interpret the massive gluons of $SU(3)_{ve}$ as coherent oscillations between neutrino states, as discussed in [[24], Ch. 9] in the context of quarks. In this case they should not be counted as relativistic degrees of freedom. It follows that runs 5 to 8 of **Table 7** are most relevant since they do not include massive gluons in such degrees of freedom. Given the arguments of this and the previous paragraph, the results of **Table 7** show consistency with both BBN observations and measurements of the Z^0 linewidth.

The primary inconsistency of the hypothesis with BBN observations identified in this section is that of D/H, the relative deuterium abundance. The calculated values of D/H under the $SU(3)_\nu$ hypothesis range from 5.7 to 10.6 × 10^{-5} in **Table 7**. These higher values of D/H are expected when neutrino generations are added to BBN calculations [41]. These values for D/H are less than those measured on earth [65] and in comets [66]. It is believed that the high values in comets likely arise from a fractionation or concentration process [67]. The outer atmosphere of Jupiter has also been measured [68] and shows a deuterium concentration D/H of 2.4 ± 0.4 × 10^{-5}. These numbers all correspond to matter that have been subject to 13 billion years of deuterium destruction, and yet all are about the same or higher than the current estimate of primordial gas-phase D/H, 2.53 ± 0.03 × 10^{-5} [64] from early gas clouds. This observational value is in good agreement with calculational estimates of neutral gas-phase D/H given in [69]. Both these papers note that depletion of deuterium onto dust and preferential incorporation into molecules could cause scatter in D/H between quasar sightlines at fixed metallicity. Cool dense gas clouds produced by stellar means will typically have conversion of atomic O and H to molecular forms in about 10^5 years after formation [70]. At gas temperatures of 4100 to 8800 K (0.35 to 0.76 eV/k) corresponding to the temperatures of the measured D/H [64], molecular species such as D_2O with an O-D bond energy of about 5 eV are likely to be present in significant quantities for the measured gas clouds.

The observational estimate of D/H is based on measurements in damped Lyman-α or Lyman limit gas clouds at redshifts of 2.5 to 3.06, corresponding to times of 2.0 to 2.6 Gyr after infinite redshift. This era is much later than the peak of early star formation, which occurred at redshifts of 15 to 20 [71]. Young stars are well-known to preferentially burn deuterium [72]. The quoted values of $^{16}O/H$ in [64] for all seven absorption systems are at least 7.9 × 10^{-7}, which is much higher than the primordial abundance predicted by BBN, ~0.96 × 10^{-15} or less [73]. Hence the absorption clouds studied are already likely affected by stellar production of oxygen and destruction of deuterium. Thus, these Lyman-α

measurements may better represent a lower bound on the primordial ratio of D/H. The observation that there are seven different absorption systems with similar D/H ratios may be more a consequence of similar evolution. There may also be an experimental bias due to the selection criterion of such Lyman-α clouds, e.g. they are circumgalactic media.

There is one more important question that should be answered before leaving this section, which is, "How can there be three times as many neutrinos participating in proton-neutron interactions when only the electron neutrino extended-color singlet participates in such electroweak charged current interactions?" Note that all three generations of neutrinos interact with the electron in the first line of the PMNS matrix, and these are of color green by the conventions of [24], forming a green extended-color singlet. Before and at neutrino decoupling, the neutral current interactions $e^+e^- \leftrightarrow \nu_\alpha \overline{\nu}_\alpha$ and $\nu_\beta \overline{\nu}_\beta \leftrightarrow \nu_\alpha \overline{\nu}_\alpha$ will equilibrate neutrinos of all colors and generations to equal number density, since all their mass-energies are much less than kT. Thus, to increase the number density of color green neutrinos and particularly green electron neutrinos would require a non-equilibrium process. One such process might convert higher-mass green neutrinos to the lowest-mass (electron) neutrino state (assuming the normal hierarchy). A second such process might convert red and blue electron neutrinos to green electron neutrinos, presumably also converting higher-mass green neutrinos to red or blue in order to conserve color. One instantiation of the former process are decays of mesonic neutrino states that are quasi-bound by $SU(3)_\nu$. Such states are denoted $\nu_\alpha \overline{\nu}_\beta$, where α and β index mass. The higher-mass states would then decay via $\nu_2 \overline{\nu}_2 \to \nu_1 \overline{\nu}_1 + \nu_1 \overline{\nu}_1$ and $\nu_3 \overline{\nu}_3 \to \nu_2 \overline{\nu}_2 + \nu_1 \overline{\nu}_1$, for example. This process would also create an excess of red and blue states of lowest mass, due to the colorless nature of mesons. The non-equilibrium aspect of this process would occur if the lifetime of such decays is comparable to the age of the universe at neutrino decoupling, so that at the time of significant conversion, the temperatures are so low that the reverse process cannot occur.

This section shows overall concurrence of the hypothesis with key BBN observations using both simplified formula as well as state-of-the-art BBN codes. The simplified first-order results for Y_p given by Equation (22) show good qualitative agreement with the detailed model for runs 4 and 5 of **Table 7**. The calculations for Li/H abundance show *much* better agreement with observations than the calculations using inputs from the standard cosmology. The required increase in the number of electron neutrino states to support increased neutron-proton interaction rates is quantitatively consistent with the extended-color theory and Z^0 linewidth measurements. Further calculations can and should be performed to assess this consistency. Despite these positive results, there is one important inconsistency—the latest observationally-inferred primordial deuterium abundance in the gas phase differs from the abundance computed here by many standard deviations (corresponding to a factor of 2.28). This exception

might well be addressed by reinterpretation of such D/H measurements as a lower bound, or by additional calculations or observations as suggested above.

5. Consistency of the Hypothesis with SN1987a Measurements

SN 1987A was a type II supernova in the Large Magellanic Cloud, a dwarf galaxy in the vicinity of the Milky Way. It occurred approximately 52 kpc from earth. Neutrinos were observed from SN1987a with energies up to 40 MeV [50]. Neutrinos of all three types are expected, due to charged and neutral weak current interactions such as $e^+e^- \leftrightarrow \upsilon_\alpha \overline{\upsilon}_\alpha$ and $\upsilon_\alpha \overline{\upsilon}_\alpha \leftrightarrow \upsilon_\beta \overline{\upsilon}_\beta$ ($\beta = \alpha$ for elastic interactions, $\beta \neq \alpha$ for inelastic interactions). Here β and α denote any one of the three neutrino flavors. The emitted neutrinos would need to propagate through an interstellar medium consisting of baryonic neutrinos. Given that the number of supernova neutrinos detected was within a factor of 2 of expectations [42], this sets a limit on the density of baryonic neutrinos and the cross-section of $SU(3)_v$ interactions of supernova neutrinos with baryonic neutrinos. One may assume a density of baryonic neutrinos that match that given in [23]. For example, with a baryonic neutrino mass of 0.4 eV/c^2 one finds a range of densities from about 10^{14} m^{-3} at 52 kpc from the galactic origin to about 5×10^{14} m^{-3} at earth's radius from the origin. From this, a mean density N_{bv} of baryonic neutrinos of 2×10^{14} m^{-3} is estimated along the path, and there are 3 neutrinos per baryonic neutrino. Assuming the interaction has a cross-section of the form $(f/137^2)(4\pi/3)(\hbar c)^2/s$ as in Section 2, one can estimate a decay distance given by $(N_{bv}\sigma_{v\text{-}bv})^{-1}$, where $\sigma_{v\text{-}bv}$ is the cross-section between supernova neutrinos and baryonic neutrinos. It is assumed that the supernova neutrinos from SN1987a have a mean energy of $E_1 = 7.5$ MeV [50]. Assuming a neutrino in a baryonic neutrino has an energy of about $E_2 = 0.4/3 = 0.133$ eV, and that the two velocities are perpendicular in earth's reference frame, one has that $s = 2E_1E_2 + 2(m_vc^2)^2 = 1412^2$ eV^2.

The result is shown in **Figure 3** for varying coupling strength factor f. The horizontal line in **Figure 3** indicates a decay distance of about 52 kpc, the range from SN1987a to earth. The vertical line indicates the normalized coupling factors consistent with that decay distance or greater, assuming that the loss of neutrinos is less than exp(−1). **Figure 3** indicates that the value of f for colorless baryonic neutrinos to supernova neutrinos should be no more than about 6.8×10^{-13}. Note that this is consistent with the theoretical estimates from Section 2 that are no more than 3×10^{-18}.

One might also inquire on the electroweak interaction rates of neutrinos contained in baryonic neutrinos with supernovae neutrinos and other ordinary matter. As noted in Section 2, the cross-sections σ_{ew} for electroweak interactions are of the form

$$\sigma_{ew} = c_{ew} G_{F0}^2 s (\hbar c)^2, \tag{24}$$

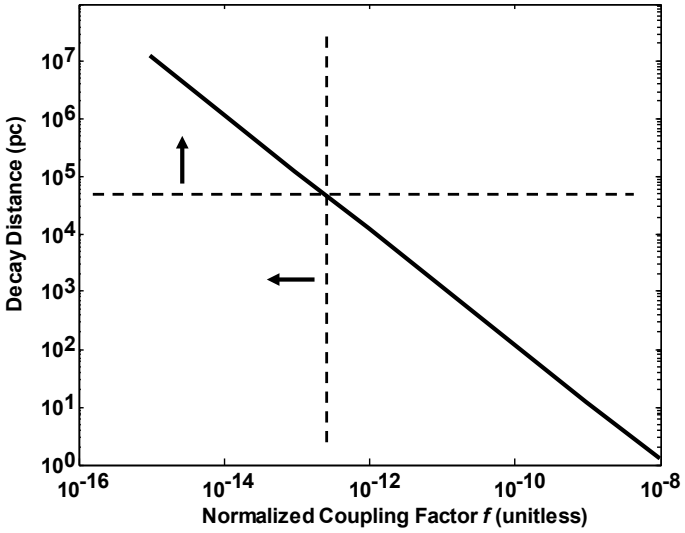

Figure 3. Decay distance (pc) of neutrinos versus baryonic neutrino coupling factor *f*, defined in Equation (1).

where c_{ew} is a coupling constant of the order of unity that depends on the specific interaction, G_{F0} is the Fermi constant defined in Section 2, and s is as defined above. For interactions between a neutrino in a baryonic neutrino and another baryonic neutrino, s is of the order of $2(0.4/3)^2 = 0.192$ eV^2, based on the discussions above. For solar neutrinos, s is of the order of 300^2 eV^2 using a solar neutrino energy of 0.3 MeV. For ordinary matter outside of supernovae, the value of s is of the order of 0.52 MeV^2 for an electron as the interaction partner. Given a mean baryonic neutrino density of 5×10^{14} m^{-3} near earth as discussed above, the density of constituent neutrinos is 1.5×10^{15} m^{-3}.

Using the above information, Table 8 recapitulates the results of Table 2 for the relevant cross-sections and interaction rates for baryonic neutrinos with ordinary matter and also includes supernova neutrinos. As can be seen from the table, such matter is indeed dark to conventional interactions if it exists, with negligible interaction rates over the age of the universe.

It is also worth noting that the current theories of neutrinos in supernovae and nuclei provide an additional upper bound on f for SU(3)$_v$. Current theories for supernovae (and other interactions such as neutron decay) assume only electroweak interactions for neutrino kinetic energies of about 1 MeV or more. Hence the value of $(4\pi/3)(f/137^2)(\hbar c)^2/s$ must be less than σ_{ew} at such center-of-mass energies or greater. This puts an upper bound on f of 6×10^{-19}. This upper bound is consistent with the range of values discussed in Section 2.

The above calculations are important in estimating the free-streaming length in the early universe. The standard paradigm with only the electroweak interaction for neutrinos after decoupling has a scattering length of the order of $(\rho\sigma_{ew})^{-1}$ that scales versus temperature T as $(T^3T^2)^{-1} = T^{-5}$ for relativistic neutrinos. This implies that the scattering length increases rapidly with decreasing temperature and neutrinos soon become free-streaming in this case. With an SU(3)$_v$ interaction

Table 8. Approximate electroweak interaction cross-sections and interaction rates of baryonic neutrinos with other forms of matter.

Form of Matter	Cross-Section (barns)	Interaction Rate (year^{-1})
Other baryonic neutrinos	$<2.2 \times 10^{-33}$	$<9.2 \times 10^{-31}$
Electrons	1.4×10^{-20}	3.9×10^{-20}
Solar neutrinos	4.2×10^{-27}	5.9×10^{-24}
Supernova neutrinos	$<1.1 \times 10^{-25}$	$<1.5 \times 10^{-22}$

Note. Assumes $c_{ew} = 1$ in Equation (23).

that scales as $1/s \sim 1/T^2$, the scattering length scales according to $(T^3 T^{-2})^{-1} = 1/T$ for relativistic neutrinos, and like $(T^{3/2} T^{-2})^{-1} = T^{1/2}$ for nonrelativistic neutrinos. This scaling implies that the posited $SU(3)_v$ interaction reduces free-streaming by neutrinos or baryonic neutrinos compared to the electroweak interaction shortly after they interact via $SU(3)_v$. This reduction is further enhanced when they become nonrelativistic, until they are bound at kinetic energies of about 0.02 eV as discussed in Section 3.

This section shows top-level consistency of the hypothesis with the available supernova neutrino data, both in terms of the interaction of neutrinos in supernovae as well as in their transport to the vicinity of earth.

6. Consistency of the Hypothesis with CMB

CMB and associated anisotropy measurements are known to explicitly provide information about the overall proportion of dark matter in the universe, and also DM annihilation rates [74]. However, inspection of recent comprehensive results [44] indicates that the CMB measurements also have quite a bit to say about the form of dark matter hypothesized herein. These include (a) the effective number of neutrino flavors before recombination, (b) the sum of neutrino masses, and (c) the helium fractional abundance. Ade *et al.* also explicitly address the possibility of massive neutrinos with masses less than 1 eV/c^2, and that it might help reconcile the lower σ_8 (the late-time fluctuation amplitude) of PLANCK compared to weak lensing measurements and the abundance of rich clusters. Note that this paper does not claim that there are massive neutrinos, i.e., with masses greater than 0.07 eV/c^2. On the contrary, it claims that low-mass neutrinos form colorless bound states that are more massive. With this in mind, the comparison to CMB results are summarized in **Table 9**. One sees that there is a high degree of consistency between recent CMB findings and this theory. The calculations of this work are quite preliminary so error bars are usually not shown. Good agreement is seen for all five of the quantities shown in the table.

7. Discussion

Straightforward calculations are performed for DM by considering an SU(3) interaction for neutrinos. Both $SU(3)_{vs}$ and $SU(3)_{ve}$ are largely consistent with observationally-inferred measurements if one allows $SU(3)_{vs}$ to have a different

Table 9. Comparison of CMB findings of [44] and this work.

Parameter	CMB	This work	Comments
DM fraction of total mass, Ω_{DM}/Ω_m	84% ± 3%	83.2% ± 8%	Computed in Section 3
Effective number of neutrino flavors, N_{eff}	3.15 ± 0.23	3.04 - 3.12	Computed in Section 3
Sum of neutrino masses, eV/c^2	<0.23	0.07	An assumed input in this work
Annihilation factor p_{ann}	$<3*10^{-28}$	0.0	cm^3 sec^{-1} Gev^{-1}
Helium fractional abundance, Y_p	0.245 ± 0.003	0.245	Computed in Section 4

strength than that for quark SU(3). This different strength and other key attributes of this force are estimated from an extension of SU(3) derived from [24] in the **Appendix**. Neutrino oscillations are direct evidence for bound neutrino states in this extension of SU(3). The theory also yields the very weak interactions expected of dark matter as shown in Section 2. The size, shape, and mass of galactic halos are derived from the theory in a companion paper [23] and are good matches to observations. There is also a match for halo interactions, specifically the Bullet Cluster interaction. That paper also shows a qualitative match to estimated dark matter properties near earth. A key past objection to neutrinos as dark matter is the large free-streaming length. This is overcome here by an SU(3) self-interaction, as shown in Section 3. The RMS streaming length is computed to range from 0.25 kpc to as much as 180 kpc, accounting for the expansion of the universe to the modern era. This is in good agreement with observed dwarf and nominal galactic halo sizes. Because of the deduced nature of this form of matter, a degenerate Fermi fluid, the halo size is expected to evolve little after initial SU(3) binding into macroscopic entities, except via aggregation. Overall, Section 3 finds that most neutrinos "hadronize" in about 300 sec or less after neutrino decoupling, become non-relativistic after about 1000 years, and then bind into macroscopic entities at about 85 kyr.

Another key objection to additional species of neutrinos (or any other form of non-sterile fermionic dark matter with mass less than 45 GeV/c^2) is the contribution to the Z^0 linewidth. As discussed in Section 3, the extended-color theory with its extra neutrino states exhibits good consistency with the QED corrected measurement of the FWHM Z^0 linewidth. This agreement arises from the property that neutrinos are extended-color singlets as they pertain to the electroweak Lagrangian density.

The presence of numerous bound neutrino species in the early universe is found to be consistent with CMB calculations, as shown in Sections 3, 4, and 6. This includes the ratio of dark matter to total matter, the effective number of neutrinos, the annihilation rate, the sum of the masses of neutrino mass eigenstates, and helium fractional abundance. As the universe cools, the presence of only a few residual bound neutrino species is consistent with observationally-inferred halo properties [23]. Such species are assumed to be fermionic and hence baryonic in this paper, as opposed to bosonic and mesonic. This is in ac-

cord with the baryonic nature of the quark sector in the modern cool universe. The calculations of Section 4 show that $SU(3)_{vs}$ may be a better fit than $SU(3)_{ve}$ for BBN parameters. The detailed calculations of the ^{7}Li/H ratio is within 1 standard deviation of the accepted value inferred from observations, and this is for both $SU(3)_{vs}$ and $SU(3)_{vs}$. This addresses an important issue in BBN physics.

The hypothesized form of DM is found to interact very weakly with ordinary matter and with free neutrinos, as discussed in Sections 2 and 5. This is because the electroweak interaction, which scales like the square of the center-of-mass energy, is extremely weak for such cold particles. Further, the proposed $SU(3)_v$ interaction strength implies that the interaction cross sections with quarks is also quite small, and quite possibly zero. The computed mean free scattering times for such interactions in the modern era are consistent with what one might expect for dark matter, *i.e.*, greater than the age of the universe in most cases. Section 5 finds consistency with available observations of supernova neutrinos, both in terms of their creation and their unobstructed transport to earth.

Perhaps most significantly, Section 3 shows good consistency between the computed and observationally-inferred values of the ratio of dark matter to other matter in the modern era. The ratio of dark matter to neutrinos, Ω_{DM}/Ω_ν, is computed as 147 versus 158 from observations. The ratio of dark matter to conventional matter, Ω_{DM}/Ω_m, is computed as 83.2% versus 84.2% from observations. These results are obtained from two independent arguments: 1) the number of species of hadronic neutrinos produced relative to residual neutrinos, and 2) pressure equilibrium between pockets of bound neutrinos in a sea of free neutrinos as the latter become nonrelativistic. The latter also relies on the assumed values of neutrino masses as well as the baryonic neutrino masses computed in the **Appendix**.

There is one primary potential *in*consistency with observations: the primordial abundance of deuterium. The most current observationally-inferred ratio for gas phase primordial D/H is about $(2.6 \pm 0.03) \times 10^{-5}$, whereas the numerical computations yield values 5.7×10^{-5} to 10.5×10^{-5} for $SU(3)_v$. These differences between computed values and observationally-inferred values for primordial D/H are not large in an absolute or a relative sense but are tremendous compared to the error bars in the latest measurements. The computed numbers are smaller than the measured values of D/H on earth and in comets. As explained in Section 4, it is possible that the observationally-inferred values do not properly account for stellar destruction or other destruction of primordial deuterium, or that there is extra "dark deuterium." With these considerations, the observationally-inferred primordial D/H may rather represent a lower bound. To a much lesser extent, there is also a potential inconsistency with observationally-inferred primordial ^{3}He/H. Until these two issues are fully resolved, the hypothesis of bound neutrinos for DM will remain yet another "modest extension" of the Standard Model, despite the many aspects of DM that are successfully explained.

8. Summary

With the assumption of a feeble form of SU(3) for neutrinos, derivable from the extended color theory as in the **Appendix**, one obtains (a) interaction rates of DM with ordinary matter that are within expectations, (b) a ratio of dark matter to neutrino energy density within 7% of current estimates, (c) a ratio of dark matter to total matter of 83.2% ± 8%, within 2% of current estimates, (d) a plausible cosmological evolution that matches BBN and CMB results within error bars, (e) a resolution to the lithium problem in standard cosmology, (f) diffusive streaming lengths consistent with current galactic halo measurements, and (g) consistency with SN1987a measurements. Consistency with Z^0 linewidth measurements are also addressed. However, the BBN analysis does *not* agree with the latest primordial deuterium measurements. The latter disagreement is the only identified potential inconsistency with current cosmological measurements.

In addition to this potential inconsistency, further work definitely remains. More quantitative values for hadronic neutrino masses and binding could be derived from $SU(3)_\nu$. The mean-free path calculations of Section 3 could be made more rigorous. More detailed calculations could be done to address the spatio-temporal evolution of the proposed form of dark matter from the time it becomes nonrelativistic to the modern era. Additional investigation regarding nucleosynthesis is warranted. More work could be done to detail the possible impact on CMB measurements, including BAO. Further observations of haloes and their interactions would provide helpful tests of the theory, as mentioned in the companion paper. There are other phenomena that are potentially related to the hypothesis of this paper, such as accelerator neutrino anomalies and cosmological baryon asymmetry, which might be explored for consistency as well.

Acknowledgements

Portions of this work were presented in Paper APR19-000356 at the 2019 April Meeting of the American Physical Society. The material of this paper represents significant improvements over that of the conference paper. The author also wishes to thank T. Slatyer, A. Nelson (deceased), S. Dodelson, A. de Gouvea, and S. Gregory for helpful discussions.

Conflicts of Interest

The author declares no conflicts of interest regarding the publication of this paper.

References

[1] White, S.D.M., Frenk, C.S. and Davis, M. (1983) *The Astrophysical Journal*, **274**, L1-L5. https://doi.org/10.1086/184139

[2] Blumenthal, G.R., Faber, S.M., Primack, J.R. and Rees, M.J. (1984) *Nature*, **311**, 517-525. https://doi.org/10.1038/311517a0

[3] Davis, M., Efstathiou, G., Frenk, C.S. and White, S.D.M. (1985) *The Astrophysical Journal*, **292**, 371-394. https://doi.org/10.1086/163168

[4] Weinberg, S. (2008) Cosmology. Oxford University Press, Oxford.

[5] Colombi, S., Dodelson, S. and Widrow, L.M. (1996) *The Astrophysical Journal*, **458**, 1-17. https://doi.org/10.1086/176788

[6] Bode, P., Ostriker, J.P. and Turok, N. (2001) *The Astrophysical Journal*, **556**, 93-107. https://doi.org/10.1086/321541

[7] Iršič, V., Viel, M., Haehnelt, M.G., Bolton, J.S., Cristiani, S., *et al.* (2017) *Physical Review D*, **96**, Article ID: 023522.

[8] Hsueh, J.-W., Enzi, W., Vegetti, S., Auger, M.W., Fassnacht, C.D., *et al.* (2019) *Monthly Notices of the Royal Astronomical Society*, **492**, 3047-3059. https://doi.org/10.1093/mnras/stz3177

[9] Hernquist, L., Katz, N., Weinberg, D.H. and Miralda-Escudé, J. (1996) *The Astrophysical Journal*, **457**, L51-L55. https://doi.org/10.1086/309899

[10] Yoshida, N., Springel, V., White, S.D.M. and Tormen, G. (2000) *The Astrophysical Journal*, **544**, L87-L90. https://doi.org/10.1086/317306

[11] Balberg, S., Shapiro, S.L. and Inagaki, S. (2002) *The Astrophysical Journal*, **568**, 475-487. https://doi.org/10.1086/339038

[12] Vogelsberger, M., Zavala, J. and Loeb, A. (2012) *Monthly Notices of the Royal Astronomical Society*, **423**, 3740-3754. https://doi.org/10.1111/j.1365-2966.2012.21182.x

[13] Shao, S., Gao, L., Theuns, T. and Frenk, C.S. (2013) *Monthly Notices of the Royal Astronomical Society*, **430**, 2346-2358. https://doi.org/10.1093/mnras/stt053

[14] Vogelsberger, M., Genel, S., Sijacki, D., Torrey, P., Springel, V., *et al.* (2013) *Monthly Notices of the Royal Astronomical Society*, **436**, 3031-3067. https://doi.org/10.1093/mnras/stt1789

[15] Vogelsberger, M., Genel, S., Springel, V., Torrey, P., Sijacki, D., *et al.* (2014) *Nature*, **509**, 7459-7531. https://doi.org/10.1038/nature13316

[16] Cyr-Racine, F.-Y., Sigurdson, K., Zavala, J., Bringmann, T., Vogelsberger, M., *et al.* (2016) *Physical Review D*, **93**, Article ID: 123527. https://doi.org/10.1103/PhysRevD.93.123527

[17] Robertson, A., Massey, R. and Eke, V. (2017) *Monthly Notices of the Royal Astronomical Society*, **467**, 4719-4730. https://doi.org/10.1093/mnras/stx463

[18] Robertson, A., Massey, R. and Eke, V. (2017) *Monthly Notices of the Royal Astronomical Society*, **465**, 569-587. https://doi.org/10.1093/mnras/stw2670

[19] Brinckmann, T., Zavala, J., Rapetti, D., *et al.* (2018) *Monthly Notices of the Royal Astronomical Society*, **474**, 746-749. https://doi.org/10.1093/mnras/stx2782

[20] Vogelsberger, M., Zavala, J., Schutz, K. and Slatyer, T.R. (2019) *Monthly Notices of the Royal Astronomical Society*, **484**, 5437-5453. https://doi.org/10.1093/mnras/stz340

[21] Tulin, S. and Yu, H.-B. (2017) *Physics Reports*, **730**, 1-58. https://doi.org/10.1016/j.physrep.2017.11.004

[22] Zavala, J. and Frenk, C.S. (2019) *Galaxies*, **7**, 81-135. https://doi.org/10.3390/galaxies7040081

[23] Holmes, R. (2020) *Journal of Modern Physics*, **11**, 854-885. https://doi.org/10.4236/jmp.2020.116053

[24] Holmes, R. (2018) A Quantum Field Theory with Permutational Symmetry. Lam-

bert Academic Press, Riga.

[25] Holmes, R. (2021) A Quantum Field Theory with Permutational Symmetry. 2nd Edition, Lambert Academic Press, Riga.

[26] Cárcamo-Hernández, A.E., Catano Mur, E. and Martinez, R. (2014) *Physical Review D*, **90**, Article ID: 073001. https://doi.org/10.1103/PhysRevD.90.073001

[27] Hati, C., Patra, S., Reig, M., Valle, J.W.F. and Vaquera-Araujo, C.A. (2017) *Physical Review D*, **96**, Article ID: 015004. https://doi.org/10.1103/PhysRevD.96.015004

[28] Singer, M., Valle, J.W.F. and Shechter, J. (1980) *Physical Review D*, **22**, 738-743. https://doi.org/10.1103/PhysRevD.22.738

[29] Tanabashi, M., Hagiwara, K., Hikasa, K., Nakamura, K., Sumino, Y., *et al.* (2018) *Physical Review D*, **98**, Article ID: 030001, Section 9.

[30] Sterman, G. and Weinberg, S. (1977) *Physical Review Letters*, **39**, 1436-1438. https://doi.org/10.1103/PhysRevLett.39.1436

[31] Tanabashi, M., Hagiwara, K., Hikasa, K., Nakamura, K., Sumino, Y., *et al.* (2018) *Physical Review D*, **98**, Article ID: 030001, b-quark mass.

[32] Tanabashi, M., Hagiwara, K., Hikasa, K., Nakamura, K., Sumino, Y., *et al.* (2018) *Physical Review D*, **98**, Article ID: 030001, t-quark mass.

[33] Tanabashi, M., Hagiwara, K., Hikasa, K., Nakamura, K., Sumino, Y., *et al.* (2018) *Physical Review D*, **98**, Article ID: 030001, Section 14.

[34] Peskin, M.E. and Schroeder, D.V. (2016) An Introduction to Quantum Field Theory. Westview Press, Boulder.

[35] Husdal, L. (2016) *Galaxies*, **4**, 78-107. https://doi.org/10.3390/galaxies4040078

[36] Weinberg, S. (2013) *Physical Review Letters*, **110**, Article ID: 241301. https://doi.org/10.1103/PhysRevLett.110.261601

[37] Tanabashi, M., Hagiwara, K., Hikasa, K., Nakamura, K., Sumino, Y., *et al.* (2018) *Physical Review D*, **98**, Article ID: 030001, Section 2.

[38] Schael, S., Barate, R., Bruneliere, R., Buskulic, D., DeBonis, I., *et al.* (2006) *Physics Reports*, **427**, 257-454. https://doi.org/10.1016/S0370-1573(05)00511-9

[39] Zyla, P.A. Barnett, R.M., Beringer, J., Dahl, O., Dwyer, D.A., *et al.* (2020) *Progress in Theoretical and Experimental Physics*, **2020**, 083C01.

[40] Berlin, A., Blinov, N. and Li, S.-W. (2019) *Physical Review D*, **100**, Article ID: 015038. https://doi.org/10.1103/PhysRevD.100.015038

[41] Pitrou, C., Coc, A., Uzan, J.-P. and Vangioni, E. (2018) *Physics Reports*, **4**, 005.

[42] Perkins, D.H. (2000) Introduction to High Energy Physics. 4th Edition, Cambridge University Press, Cambridge.

[43] Cahill, K. (2019) Physical Mathematics. Cambridge University Press, Cambridge.

[44] Ade, P.A.R., Aghanim, N., Arnaud, M., Ashdown, M. Aumont, J., *et al.* (2016) *Astronomy & Astrophysics*, **594**, A13.

[45] Aghanim, N., Akrami, Y., Ashdown, M., Aumont, J., Baccigalupi, C., *et al.* (2020) *Astronomy & Astrophysics*, **641**, A1.

[46] Schneider, A., Smith, R.E., Maccio, A.V. and Moore, B. (2012) *Monthly Notices of the Royal Astronomical Society*, **424**, 684-698. https://doi.org/10.1111/j.1365-2966.2012.21252.x

[47] Kolb, E. and Turner, M. (1990) The Early Universe. CRC Press, Boca Raton.

[48] Bond, J.R., Efstathiou, G. and Silk, J.R. (1980) *Physical Review D*, **45**, 1980-1984. https://doi.org/10.1103/PhysRevLett.45.1980

[49] Bond, J.R. and Szalay, A.S. (1983) *The Astrophysical Journal*, **274**, 443-468. https://doi.org/10.1086/161460

[50] Janka, H.-T. (2017) Neutrino Emission from Supernovae. In: Alsabti, A. and Murdin, P., Eds., *Handbook of Supernovae*, Springer, Cham, 1575-1604.

[51] Burrows, A., Reddy, S. and Thompson, T.A. (2006) *Nuclear Physics A*, **777**, 356-394. https://doi.org/10.1016/j.nuclphysa.2004.06.012

[52] Tanabashi, M., Hagiwara, K., Hikasa, K., Nakamura, K., Sumino, Y., *et al.* (2018) *Physical Review D*, **98**, Article ID: 030001, Section 23, "BBN".

[53] Bernstein, J., Brown, L.S. and Feinberg, G. (989) *Reviews of Modern Physics*, **61**, 25-39. https://doi.org/10.1103/RevModPhys.61.25

[54] Alpher, R.A. and Herman, R.C. (1950) *Reviews of Modern Physics*, **22**, 153-212. https://doi.org/10.1103/RevModPhys.22.153

[55] Hayashi, C. (1950) *Progress of Theoretical Physics*, **5**, 224-235. https://doi.org/10.1143/ptp/5.2.224

[56] Peebles, P.J.E. (1966) *The Astrophysical Journal*, **146**, 542-552. https://doi.org/10.1086/148918

[57] Wagoner, R.V., Fowler, W.A. and Hoyle, F. (1967) *The Astrophysical Journal*, **148**, 3-50. https://doi.org/10.1086/149126

[58] Peebles, P.J.E. (1971) Physical Cosmology. Princeton University Press, Princeton.

[59] Steigman, G.D., Schramm, N. and Gunn, J.E. (1977) *Physics Letters B*, **66**, 202-204. https://doi.org/10.1016/0370-2693(77)90176-9

[60] Sarkar, S. (1996) *Reports on Progress in Physics*, **59**, 1493-1610. https://doi.org/10.1088/0034-4885/59/12/001

[61] Olive, K.A. and Skillman, E. (2004) *The Astrophysical Journal*, **617**, 29-49. https://doi.org/10.1086/425170

[62] Fields, B.D. (2011) *Annual Review of Nuclear Particle Science*, **61**, 47-68. https://doi.org/10.1146/annurev-nucl-102010-130445

[63] Cyburt, R.H., Fields, B.D., Olive, K.A. and Yeh, T.-H. (2016) *Reviews of Modern Physics*, **88**, Article ID: 015004. https://doi.org/10.1103/RevModPhys.88.015004

[64] Cooke, R.J., Pettini, M. and Steidel, C.C. (2018) *The Astrophysical Journal*, **855**, A102. https://doi.org/10.3847/1538-4357/aaab53

[65] Hagemann, R., Nief, G. and Roth, E. (1970) *Tellus*, **22**, 712-715. https://doi.org/10.3402/tellusa.v22i6.10278

[66] Altwegg, K., Balsiger, H., Bar-Nun, A., Berthelier, J.J., Bieler, A., *et al.* (2015) *Science*, **347**, Article ID: 1261952. https://doi.org/10.1126/science.1261952

[67] Vanysek, V. and Vanysek, P. (1984) *Icarus*, **61**, 57-59. https://doi.org/10.1016/0019-1035(85)90154-X

[68] Lellouch, E., Bézard, B., Fouchet, T., Feuchtgruber, H., Encrenaz, T., *et al.* (2001) *Astronomy & Astrophysics*, **670**, 610-622. https://doi.org/10.1051/0004-6361:20010259

[69] van de Voort, F., Quataert, E., Faucher-Giguére, C.-A., Kereš, D., Hopkins, P., *et al.* (2018) *Monthly Notices of the Royal Astronomical Society*, **477**, 80-92. https://doi.org/10.1093/mnras/sty591

[70] Wirström, E.S., Charnley, S.B., Cordiner, M.A. and Ceccarelli, C. (2016) *The Astrophysical Journal*, **830**, 102-106. https://doi.org/10.3847/0004-637X/830/2/102

[71] Klessen, R.S. (2018) Formation of the First Stars. In: Latif, M. and Schleicher, D.R.G., Eds., *Formation of the First Black Holes*, World Scientific Publishing, Sin-

gapore, 67.

[72] Adams, F.C. (2020) Chapter 5: The Origin of Stars and Planets. In: Malkan, M.A. and Zuckerman, B., Eds., *Origin and Evolution of the Universe*, 2nd Edition, World Scientific Publishing, Singapore, 149.

[73] Coc, A. and Vangioni, E. (2017) *International Journal of Modern Physics E*, **26**, Article ID: 1741002. https://doi.org/10.1142/S0218301317410026

[74] Giesen, G., Lesgourgues, J., Audren, B. and Haimoud, A. (2012) *Journal of Cosmology and Astroparticle Physics*, **12**, 008. https://doi.org/10.1088/1475-7516/2012/12/008

Appendix. Estimate of Binding Energy of Hadronic Neutrinos and $SU(3)_{ve}$ Interaction Strength

This Appendix estimates the binding energy of baryonic and mesonic neutrinos as well as the $SU(3)_{ve}$ interaction strength for relativistic neutrinos. Because the SU(3) binding energy is a large fraction of the mass-energy of bound quarks, one might expect that this would be the case for SU(3)-bound neutrinos as well (should they exist). This fact is utilized for estimation of the mass-energy of bound neutrino states.

The binding energy of baryonic neutrinos is estimated first. From equation (10.27a) of [24], the binding energy E_b of a baryonic neutrino can be approximated by

$$E_b = \beta_{\upsilon\tau}^2 \left(\hbar c/4\right)\left\{4\pi\alpha_3 \left(m_{\upsilon e}^2 + m_{\upsilon\mu}^2 + m_{\upsilon\tau}^2\right)^{1/2} c^2/\left(\hbar c\right)\right\}^2 \left|\Delta x\right|, \tag{A1}$$

where $\beta_{\upsilon\tau}^2$ is the probability of the highest-mass tau neutrino and α_3 is the dimensionless coupling parameter for the strong force, $g_s^2/\left(4\pi\hbar c\right)$. The neutrino masses are denoted by $m_{\nu e}$, $m_{\nu\mu}$, and $m_{\nu\tau}$ (the naming convention implicitly assumes the normal mass hierarchy). The length $|\Delta x|$ is the characteristic size of an SU(3)-bound neutrino. The value of α_s is chosen to equal 1 in this calculation because for bound SU(3) states the coupling parameter is close to 1 for quark-quark interactions, and that should apply here as well. The probability of an upper-mass neutrino state from the same reference for a marginally relativistic bound state is given by

$$\beta_{\upsilon\tau}^2 = m_{\upsilon e}/\left(m_{\upsilon e} + m_{\upsilon\tau}\right) \tag{A2}$$

This probability is approximately 0.1 for $m_{\nu e} \sim 0.005$ eV/c^2 and $m_{\nu\tau} \sim 0.05$ eV/c^2, assuming the normal hierarchy for neutrino masses, the known mass-squared differences, and the least possible mass for the tau neutrino. Under the same assumptions, the muon neutrino mass is about 0.01 eV/c^2. The last input to Equation (A1) is the characteristic size of SU(3)-bound neutrinos. For this, use an estimate based on the Heisenberg uncertainty principle, again assuming a marginally relativistic state:

$$\left|\Delta x\right| \geq \hbar c/\left(pc\right) \approx \hbar c/\left(m_{\upsilon\tau}c^2\right). \tag{A3}$$

Using the nominal value of $m_{\nu\tau}$ given above, one obtains $|\Delta x| \sim 3.3$ microns. One might also use $m_{\nu e}$ or $m_{\nu\mu}$ in Equation (A3), but the basis of Equation (A1) suggests that $m_{\nu\tau}$ should be used. Substituting the above into Equation (A1), one obtains an estimate of the binding energy of baryonic neutrinos.

$$E_b \geq 4\pi^2 m_{\upsilon e}c^2 = 0.2 \text{ eV}. \tag{A4}$$

One can see that with these approximations and assumptions, the binding energy is roughly independent of the upper neutrino mass value. In Equation (A3), one might also use $\left(m_{\upsilon\tau}m_{\upsilon e}\right)^{1/2}c^2$ for the denominator based on Ch. 10 of [24]. With this assumption, one obtains

$$E_b \approx 4\pi^2 m_{\upsilon e}c^2\left(m_{\upsilon\tau}/m_{\upsilon e}\right)^{1/2} = 4\pi^2\left(m_{\upsilon\tau}m_{\upsilon e}\right)^{1/2}c^2 = 0.62 \text{ eV}. \tag{A5}$$

To this range of binding energies, 0.2 to 0.63 eV, one must add the contribution of the masses of the constituent neutrinos, which might range from $3m_{ve}$ to $3m_{v\tau}$. This then leads to a range of baryonic neutrino masses from about 0.22 eV/c^2 to about 0.8 eV/c^2. Assuming the baryonic neutrinos comprise the lower-mass neutrino states as in quarks, a tighter range would be 0.22 to 0.64 eV/c^2. On the other hand, a baryonic neutrino mass as high as 0.8 eV/c^2 should not immediately be ruled out. Equation (10.27b) of [24] gives a similar equation for mesonic neutrino states, and the corresponding range of masses is 0.08 to 0.35 eV/c^2.

The above mass-scaling analysis can also be applied to relativistic particles using Equation (10.13b) rather than (10.13a) of [24]. In this limit, $\beta_{v\tau}^2 \sim 0.5$, independent of the underlying masses. Referring to Equation (A1) and removing the $|\Delta x|$ to obtain the interaction force coupling parameter, one finds that the interaction scales as $m_{v\tau}^2$ in this case. This justifies a scaling of the interaction strength for relativistic particles from quarks to neutrinos by $\left(m_{\upsilon\tau}/m_b\right)^2$ to $\left(m_{\upsilon\tau}/m_t\right)^2$ where m_b is the bottom quark mass and m_t is the top quark mass. Note that the scaling factor between the down-quark family and up-quark family should be of order 1 because all hadrons bound by a strong quark interaction have sufficient energy for the presence of both $u-\overline{u}$ and $d-\overline{d}$ sea quarks.